N° d'ordre : *ECL 2000-08*

THESE

présentée devant

L'ECOLE CENTRALE DE LYON

ECOLE DOCTORALE : Matériaux

pour obtenir le grade de

DOCTEUR

Spécialité : Génie des Matériaux

par

Wenbin LIN

Développement de capteurs à fibre optique basés sur la résonance de plasmon de surface pour la détection physique, chimique et biologique

---

Soutenue le 16 mars 2000 devant la Commission d'Examen :

Henri GAGNAIRE	Professeur à l'Université Jean Monnet, Saint-Etienne	Président
Pierre BENECH	Professeur à LEMO, ENSERG-INPG, Grenoble	Rapporteur
Olivier PARRIAUX	Professeur à l'Université Jean Monnet, Saint-Etienne	Rapporteur
Jean-Marc CHOVELON	Professeur à l'Université Claude Bernard-Lyon1	
Nicole JAFFREZIC	Directeur de Recherche au CNRS	

P-3

N° d'ordre : *ECL 2000-08*

THESE

présentée devant

L'ECOLE CENTRALE DE LYON

ECOLE DOCTORALE : Matériaux

pour obtenir le grade de

DOCTEUR

Spécialité : Génie des Matériaux

par

Wenbin LIN

Développement de capteurs à fibre optique basés sur la résonance de plasmon de surface pour la détection physique, chimique et biologique

---

Soutenue le 16 mars 2000 devant la Commission d'Examen :

Henri GAGNAIRE	Professeur à l'Université Jean Monnet, Saint-Etienne	Président
Pierre BENECH	Professeur à LEMO, ENSERG-INPG, Grenoble	Rapporteur
Olivier PARRIAUX	Professeur à l'Université Jean Monnet, Saint-Etienne	Rapporteur
Jean-Marc CHOVELON	Professeur à l'Université Claude Bernard-Lyon1	
Nicole JAFFREZIC	Directeur de Recherche au CNRS	

ECOLE CENTRALE DE LYON
LISTE DES PERSONNES HABILITEES A ENCADRER DES THESES
Arrêté du 30.03.92 (Art. 21) et Arrêté du 23.11.88 (Art.21)
MISE A JOUR du 02.09.99

Directeur : Jean DOREY
Directeur Adjoint - Directeur des Etudes: Léo VINCENT
Directeur Administration de la Recherche : Francis LEBOEUF

LABORATOIRE	NOM-PRENOM	GRADE
CENTRE DE GENIE ELECTRIQUE DE LYON : CEGELY UPRESA 5005	AURIOL Philippe NICOLAS Alain THOMAS Gérard BEROUAL Abderrahmane CLERC Guy KRAHENBUHL Laurent NICOLAS Laurent	PROFESSEUR ECL - - - - - - MAITRE DE CONFERENCES ECL - - - DIRECTEUR DE RECHERCHE CNRS CHARGE DE RECHERCHE CNRS
EQUIPE ANALYSE NUMERIQUE LYON-ST ETIENNE UMR 5585	CHEN Liming MARION Martine MAITRE Jean-François MOUSSAOUI Mohand Arezki MUSY François	PROFESSEUR ECL - - - - - - - - - MAITRE DE CONFERENCES ECL
ICTT	DAVID Bertrand KOULOUMDJIAN M. France	PROFESSEUR ECL PROFESSEUR LYON I
INGENIERIE ET FONCTIONNALISATION DES SURFACES IFOS UMR 5621	CHAUVET Jean- Paul GUIRALDENQ Pierre MARTELET Claude MARTIN Jean-René TREHEUX Daniel VANNES Bernard VINCENT Léo CHOVELON Jean-Marc LANGLADE-BOMBA Cécile NGUYEN Du SALVIA Michelle STREMSDOERFER Guy HERRMANN Jean-Marie JAFFREZIC Nicole PICHAT Pierre CHATEAUMINOIS Antoine SOUTEYRAND Elyane JUVE Denyse	PROFESSEUR ECL - - - - - - - - - - - - - - - - - - MAITRE DE CONFERENCES ECL - - - - - - - - - - - - DIRECTEUR RECHERCHE CNRS - - - - - - CHARGE DE RECHERCHE CNRS - - - INGENIEUR DE RECHERCHE

ECOLE CENTRALE DE LYON
LISTE DES PERSONNES HABILITEES A ENCADRER DES THESES
Arrêté du 30.03.92 (Art. 21) et Arrêté du 23.11.88 (Art.21)
MISE A JOUR du 02.09.99

LABORATOIRE	NOM - PRENOM	GRADE
LABORATOIRE DE MECANIQUE DES FLUIDES ET ACOUSTIQUE LMFA UMR 5509	MATHIEU Jean	PROFESSEUR EMERITE
	ARQUES Philippe	PROFESSEUR ECL
	BRUN Maurice	- -
	CHAMPOUSSIN Jean-Claude	- -
	COMTE-BELLOT Geneviève	- -
	JEANDEL Denis	- -
	JUVÉ Daniel	- -
	LEBOEUF Francis	- -
	PERKINS Richard	- -
	ROGER Michel	- -
	SCOTT Jean	- -
	GALLAND Marie-annick	MAITRE DE CONFERENCES ECL
	BATAILLE Jean	PROFESSEUR LYON I
	BUFFAT Marc	- -
	GAY Bernard	- -
	GENCE Jean-Noël	- -
	LANCE Michel	- -
	SUNYACH Michel	- -
	BEN HADID Hamda	MAITRE DE CONFERENCES LYON I
	HAMADICHE Mahmoud	- -
	MOREL Robert	PROFESSEUR INSA
	BERTOGLIO Jean-Pierre	DIRECTEUR DE RECHERCHE CNRS
	BLANC-BENON Philippe	- -
	CAMBON Claude	- -
	ESCUDIÉ DANY	CHARGE DE RECHERCHE CNRS
	FERRAND Pascal	- -
	HENRY Daniel	- -
	LE PENVEN Lionel	- -
GSI	AIT EL HADJ Smaïl	PROFESSEUR ECL

Le travail, présenté dans ce mémoire, a été effectué dans le cadre d'une collaboration entre le laboratoire d'Ingénierie et de Fonctionnalisation des Surfaces de l'Ecole Centrale de Lyon et le laboratoire de Traitement du Signal et Instrumentation de l'Université Jean Monnet à Saint-Etienne.

J'exprime mes plus chaleureux remerciements à ma directrice de thèse Madame Nicole JAFFREZIC-RENAULT, directeur de recherche CNRS et directeur adjoint de laboratoire, qui m'a choisi parmi de nombreux candidats du CNOUS et m'a amené dans ce domaine multidisciplinaire. Elle m'a toujours encouragé et accordé un soutien efficace au long de ces trois années de thèse. Toutes mes publications sont corrigées mot par mot par sa propre main. Sans sa confiance et son expérience précieuse, cette étude aurait apporté beaucoup moins de résultats.

Il m'est particulièrement agréable de présenter ma gratitude à Monsieur Jean-Marc CHOVELON, actuellement professeur à l'Université Claude Bernard Lyon 1, Madame Monique LACROIX de ce laboratoire qui ont contribué à ce travail et m'ont apporté l'assistance indispensable pour la partie chimique. Toute ma reconnaissance pour leur amitié et leur disponibilité permanente.

Je remercie tout spécialement Monsieur le professeur Henri GAGNAIRE au laboratoire de Traitement du Signal et Instrumentation de l'Université Jean Monnet à Saint-Etienne, et les membres de son laboratoire Madame Colette VEILLAS et Messieurs Alain TROUILLET et Frédéric CELL, pour m'avoir accepté de travailler dans le cadre de notre collaboration et de m'aider à démarrer cette étude. J'ai beaucoup apprécié leurs compétences et leur sympathie. Qu'ils trouvent ici le témoignage de ma sincère reconnaissance.

Je tiens à remercier Monsieur le professeur Jean Rene MARTIN ainsi que Messieurs Denis DESCHATRE et Jean-Marc KRAFFT pour leur patience, cordialité et compétence à résoudre les difficultés expérimentales. Je suis aussi reconnaissant envers Monsieur le professeur Claude MARTELET du laboratoire pour sa gentillesse et sa disponibilité à répondre mes questions.

Je ne saurais oublier aussi Messieurs Alain GAGNAIRE, maître de conférences au laboratoire d'Electronique Optoélectronique et Microsystèmes, Pierre DUTRUC, responsable du service informatique de l'Ecole Centrale de Lyon et Jean-Michel VERNET technicien au laboratoire de Matériaux, Mécanique Physique, pour leurs disponibilités diverses et exceptionnelles. Que tous les personnels qui ont contribué de près ou de loin à ce travail et les étudiants avec qui j'ai passé de bons moments, soient sûrs de ma profonde gratitude.

Mon séjour en France a été financé par le gouvernement chinois. J'associe à ces remerciements le Service de l'Education de l'Ambassade de CHINE en France et le CROUS de Lyon - Saint-Etienne qui gèrent ma bourse.

Je dédie ce mémoire à ma femme, Xin MA, qui est toujours à mes côtés et m'apporte son soutien. La rédaction de mes publications dépend aussi de ses efforts.

Je remercie également Monsieur Henri GAGNAIRE qui m'a fait l'honneur de présider le jury de ma thèse ainsi que Messieurs Olivier PARRIAUX et Pierre BENECH qui ont bien voulu accepter d'être rapporteurs de cette étude. La participation au jury et l'appréciation de Monsieur Jean-Marc CHOVELON me font aussi particulièrement honneur.

SOMMAIRE

Développement d'un capteur à fibre optique basé sur la résonance de plasmon de surface sur film d'argent pour le suivi des milieux aqueux.

Résumé

Développement de Capteurs à Fibre Optique Basés sur la Résonance de Plasmon de Surface pour la détection Physique, Chimique et Biologique

Il est bien connu que la résonance de plasmon de surface (SPR) d'une onde électromagnétique de surface peut être utilisée en tant que sonde optique sensible à de faibles variations intervenant à l'interface métal/diélectrique. La configuration de Kreschmann basée sur un prisme est traditionnellement employée pour exciter et détecter le phénomène SPR. En 1993, le premier capteur SPR à fibre optique a été réalisé par R.C. Jorgenson et S.S. Yee et a été ensuite commercialisé par la société Biacore (Suède). Le capteur SPR à fibre optique présente un certain nombre d'avantages sur le système Kreschmann tels que sa faible taille, son faible coût et la possibilité de détection déportée. Un capteur SPR à fibre optique multimodale plus simple, utilisant l'injection oblique d'une lumière monochromatique collimatée, a été développé au laboratoire TSI de l'université Jean-Monnet de Saint-Etienne, en 1996. Utilisant l'argent pour induire le phénomène SPR d'une lumière à la longueur d'onde 670 nm, le capteur à fibre optique est un réfractomètre fonctionnant dans la gamme d'indice optique 1,35-1,40.

Ce mémoire de thèse est constitué de cinq articles visant à développée ce type de capteur à fibre optique pour les applications physique, chimique et biologique. Le premier article traite de la modification de la gamme d'indice mesurable, afin d'être capable de fonctionner dans des systèmes chimiques et biologiques, dont les indices de réfraction sont compris entre 1,33 et 1,36. Les relations entre les paramètres de structure et de matériau, de la configuration multicouche pour l'excitation du SPR, ont été déduites de la théorie. La technique sol-gel est utilisée pour fabriquer un revêtement d'acétate de zirconium de quelques dizaines de nanomètres. La fiabilité est augmentée par une protection constituée d'une monocouche auto-assemblée de thiol longue chaîne qui empêche l'oxydation de l'argent. Ce premier article a été soumis à la revue Thin Solid Films. Les variations spatiales du vecteur champ électrique au cours de la propagation des rayons non méridiens dans la fibre multimodale sont étudiées dans le second article accepté pour publication dans la revue Sensors and Actuators A. Un modèle 3D précis a été établi permettant d'expliquer le phénomène expérimental observé sur

l'influence de la direction de polarisation de la lumière incidente par rapport à la face d'entrée de la fibre. Les signaux du capteur provenant de l'adsorption d'une très fine couche diélectrique sur la surface du métal ou d'une très faible variation de l'indice de réfraction dans le milieu de mesure peuvent alors être interprétés quantitativement. L'article suivant, accepté pour publication à la revue Applied Optics, propose une méthode directe pour déterminer l'épaisseur et les constantes optiques d'un film mince de métal déposé sur le cœur de la fibre, par simple mesure de la réponse du capteur à fibre optique. L'intérêt de ce travail vient des difficultés rencontrées dans la caractérisation des films métalliques avec des surfaces courbes en utilisant des techniques optiques conventionnelles telles que la réflectométrie et l'ellipsométrie. Un nouveau moyen optique capable de suivre in-situ la formation d'une monocouche auto-assemblée d'alkylthiol est présenté dans le quatrième article, soumis au Journal of Chemical Physics. L'application de la technique SPR à fibre optique pour étudier les monocouches auto-assemblées, l'observation directe et la description du phénomène d'inclinaison des chaînes lors de l'auto-assemblage de la monocouche d'alkylthiol, à notre connaissance, n'a jamais été rapporté auparavant dans la littérature. La bonne sensibilité observée montre que notre approche du système à fibre optique est plus adaptée que l'ellipsométrie et que le système SPR à prisme pour suivre les variations sur la totalité d'un film diélectrique. Le dernier article, soumis au Japanese Journal of Applied Physics, est consacré au développement d'un biocapteur basé sur le système à fibre optique pour suivre des interactions entre biomolécules. Avec une très simple configuration, cet immunocapteur a montré de bonnes performances en sensibilité et en spécificité, comparé à l'appareil commercialisé par Biacore qui est beaucoup plus complexe et cher. Ce travail constitue un excellent départ vers le développement d'une immunosonde pour des immunoessais sans marqueur.

Ces cinq articles sont indépendants mais complémentaires l'un de l'autre. Les conditions pour lesquelles le SPR peut être excité sur une géométrie multicouche, obtenues dans le premier article, fournissent une base théorique pour le choix de la longueur d'onde de la lumière ou pour la gamme d'indice du milieu environnant lorsque l'or est utilisé et se retrouve dans les autres articles. Les études du modèle 3D précis, présenté dans le second article, pour simuler les performances des capteurs à fibre optique, permettent ensuite de caractériser le film métallique (dans le troisième article), la couche chimique adsorbée (dans le quatrième article) et les couches biomoléculaires (dans le cinquième article). De plus, la mesure des propriétés du film métallique dans le troisième article, permet de détecter avec succès, la monocouche auto-assemblée d'alkylthiol adsorbée sur la surface du métal (en référence au

quatrième article). Les déterminations des caractéristiques du film d'or et de la couche de thiol sont nécessaires pour caractériser le film d'anticorps et la couche d'anticorps-antigène après la réaction d'affinité. Un biocapteur basé sur un système SPR à fibre optique a donc été réalisé et est présenté dans le cinquième article. Ce biocapteur a été conçu, élaboré et caractérisé couche par couche.

Preface

Developments of the Fiber-Optic Sensors Based on Surface Plasmon Resonance for Physical, Chemical and Biological Detection

It is well known that surface plasmon resonance (SPR) of the surface electromagnetic wave can be used as a sensitive optical probe to the slight variations occurring in the proximity of the metal/dielectric interface. The prism-based Kretschmann configuration is traditionally employed to excite and detect the SPR. In 1993, the first fiber-optic based SPR sensor was realized by R.C.Jorgenson and S.S.Yee and then commercialized by Biacore Company (Sweden). The SPR fiber-optic sensor offers a number of advantages such as small size, low cost and feasibility in remote sensing over the bulk Kretschmann system. A simpler SPR multimode fiber-optic sensor using oblique injection of the collimated monochromatic light has been developed at the TSI laboratory, Jean Monnet University in Saint-Etienne, France since 1996. Using silver to support SPR at the light wavelength of 670nm, this fiber-optic sensor was characterized as a refractometer operating in the index range of 1.35-1.40.

This dissertation consists of five articles aimed to develop this kind of fiber-optic sensor for physical, chemical and biological applications. The first article is devoted to drop down the range of measurable indices in order to be capable of performing in most practical chemical and biochemical systems whose refractive indices are 1.33-1.36. The relations between the structural and material parameters of the multilayered configuration for the excitation of SPR at certain wavelength have been theoretically derived. Sol-gel technique is applied to fabricate the Zirconium acetate overlay as thin as some ten nanometers. The reliability is improved by preventing the oxidation of silver using a self-assembled monolayer (SAM) of long chain acid thiol. This article has been submitted to Thin Solid Films. Accepted by Sensors & Actuators A, the spatial variations of the electric field vector during the propagation of the skew rays in the multimode fiber are investigated in the second article. An accurate 3D model has been established so that the experimental phenomena, which first demonstrate the influences of the polarization direction of the incident light with respect to the input end face of the fiber, can be consistently explained. The sensing signals coming from such as the adsorption of a very thin dielectric layer on metal surface or the slight variation of the refractive index in the monitored bulk medium are ready to be quantitatively

interpreted. Next article, accepted for publication by Applied Optics, proposes a direct method to determine the thickness and the optical constants of the thin metal films deposited on the surface of the fiber core by simple measurements of fiber-optic SPR responses. The significance of this work comes from the difficulties in characterizing the metal films with curved surfaces by using the conventional optical techniques such as reflectometry and ellipsometry. A novel optical means capable of monitoring the formation process of the alkylthiol SAM is presented in the fourth article, submitted to Journal of Chemical Physics. The application of the fiber-optic SPR technique to study SAMs and the direct observation and description of the tilting process during the self-assembly of alkylthiol, to our knowledge, have never been reported before in the literature. The rather high sensitivity proves that our fiber-optic approach is more adapted than ellipsometry and the prism-based SPR system to monitor the variations over entire investigated dielectric film. Last article, submitted to Japanese Journal of Applied Physics, is dedicated to develop a biosensor based on this fiber-optic arrangement to monitor the biomolecular interaction. With very simple configuration, this immunosensor has manifested good performances in both sensitivity and specificity compared to the commercialized BIACORE Probe that is much more complex and expensive. This work makes a starting progress towards the development of a portable immunoprobe for non-labeling immunoassay.

These five articles are independent as well as supplementary each other. The conditions on which the SPR can be excited in a multilayered geometry, obtained in the first article, provide a theoretical basis for the choice of light wavelength or the index range of environment medium while metal gold is used as it can be seen in other articles. The studies of the accurate 3D model in the second article for simulating the performances of the fiber-optic sensors enable to characterize afterwards the metal film (in the third article), the chemical adsorbed layer (in the fourth article) and the functional biomolecular layers (in the 5^{th} article). Moreover, the successful measurement of the metallic film properties in the third article ensures the success in the detection of the alkylthiol SAM, which is adsorbed on the metal surface (referred to the fourth article). Furthermore, the determinations of the gold film and the thiol layer are necessary for characterizing the antibody film and the antibody-antigen-binding layer after the affinity reaction. As a result, a new SPR multimode fiber-optic biosensor has been realized and reported in the 5^{th} article. This biosensor has been well designed, elaborated and characterized at the level of its each layer.

Résumé Article 1

Développement d'un capteur à fibre optique basé sur la résonance de plasmon de surface sur film d'argent pour le suivi des milieux aqueux.

Un capteur simple à fibre optique multimodale, basé sur la résonance de plasmon de surface (SPR), a été développé au laboratoire TSI de l'université Jean-Monnet à Saint-Etienne en 1996 [1]. L'argent a été choisi comme support de la résonance de plasmon de surface, excitée par la lumière de longueur d'onde 670 nm, émise par une diode laser. Malheureusement, bien que l'argent puisse produire des résonances très fines, c'est un matériau très réactif et il peut s'oxyder dés qu'il est exposé à l'air et encore plus facilement s'il est exposé à l'eau. Ce capteur à fibre optique permettant de mesurer un indice optique dans la gamme de 1,35 à 1,40 [1], il n'est pas utilisable pour la mesure dans un environnement aqueux dont l'indice de réfraction est compris entre 1,33 et 1,36. Cette limitation empêche son utilisation pratique dans la plupart des systèmes chimiques et biochimiques.

Cet article est consacré au développement d'un capteur SPR à fibre optique recouvert d'un film d'argent, qui soit adapté aux applications chimiques et biologiques. Une monocouche auto-assemblée (SAM) de thiol longue chaîne, recouvrant la surface de l'argent, permet d'éviter la détérioration du film d'argent. Les études expérimentales montrent que par ce procédé, on augmente la durée de vie du capteur de quelques jours à quelques semaines. La gamme de mesure de l'indice de réfraction est abaissée en effectuant un recouvrement de la couche de thiol par de l'acétate de zirconium (noté ZrO_2). Des analyses théoriques ont permis de prédire la faisabilité de la configuration et les performances du capteur ont pu être simulées. Le modèle théorique développé est aussi utilisable pour la conception d'autres capteurs SPR à fibre optique ou à prisme, pour différentes applications. La technique sol-gel est utilisée pour l'élaboration du recouvrement de ZrO_2 avec une épaisseur de l'ordre de dix nanomètres. Les capteurs à fibres optiques réalisés fonctionnent effectivement dans les milieux aqueux dans une gamme d'indice de réfraction entre 1,33 et 1,36. Ce travail constitue une base pour le développement d'un capteur d'affinité.

Références: 1. C.Ronot-Trioli, A.Trouillet, C.Veillas, A.El-Shaikh and H.Gagnaire, Fibre optic chemical sensor based on surface plasmon monochromatic excitation, Analytica Chimica Acta, 319(1996) 121-127

Preface to Article 1

Development of a Fiber-Optic Sensor Based on Surface Plasmon Resonance on Silver Film for Monitoring Aqueous Media

A simple surface plasmon resonance (SPR) multimode fiber-optic sensor using oblique injection of the collimated light has been developed at the TSI laboratory, Jean Monnet University in Saint-Etienne, France since 1996[1]. Silver is selected to support the SPR excited by light of 670nm wavelength emitted from a laser diode. Unfortunately, although silver can provide the sharpest SPR, it is very active and is oxidized as soon as it is exposed to air and especially to water. Moreover, this fiber-optic sensor, having its measurable index range of about 1.35-1.40[1], is still not capable of monitoring aqueous environment whose refractive index is 1.33-1.36. This limitation prevents its uses in most practical chemical and biochemical systems.

This paper is contributed to develop a reliable fiber-optic SPR sensor based on silver aimed to chemical and biological applications. A self-assembled monolayer (SAM) of long chain thiol is introduced to cover the surface of silver in order to prevent the deterioration of silver film. Experimental studies demonstrate that, by this way, the lifetime of this sensor increases from some days to some weeks. The range of measurable indices is dropped down by coating an overlay of zirconium acetate (marked as ZrO_2) on the surface of the thiol SAM. The feasibility has been investigated in advance by the theoretical analyses and the performances of the sensor can be foresighted by the simulations. This theoretical model is also helpful to design other SPR sensors in fiber optic or in prism for different purposes. The sol-gel technique is applied to fabricate the ZrO_2 overlay as thin as some ten nanometers. The experimental fiber-optic sensors demonstrate their capability to operate in the aqueous mediums with the detectable range of refractive indices of 1.33-1.36. This work provides a base for developing an affinity biosensor.

References

1. C.Ronot-Trioli, A.Trouillet, C.Veillas, A.El-Shaikh and H.Gagnaire, Fibre optic chemical sensor based on surface plasmon monochromatic excitation, Analytica Chimica Acta, 319(1996) 121-127

Development of a Fiber-Optic Sensor Based on Surface Plasmon Resonance on Silver Film for Monitoring Aqueous Media

Wen Bin LIN[a,c], Monique LACROIX[a], Jean Marc CHOVELON[a], Nicole JAFFREZIC-RENAULT[a,*], Alain TROUILLET[b], Colette VEILLAS[b], Henri GAGNAIRE[b]

[a] IFOS, Ecole Centrale de Lyon, 36 Avenue Guy de Collongue, BP163, 69131 Ecully Cedex, France

[b] TSI, Université Jean Monnet, 23 Rue du Dr. Paul Michelon, 42023 Saint-Etienne Cedex, France

[c] Electronic Science Department, Nankai University, Tianjin, 30071, China

[*] ***Corresponding author:*** *Tel: +33 4 72186243; Fax: +33 4 78331577; Email:Nicole.Jaffrezic@ec-lyon.fr*

Abstract: A reliable fiber-optic SPR sensor based on silver is developed in this paper for chemical and biological applications. The range of measurable indices is dropped down by coating an overlay of zirconium acetate on the silver surface by sol-gel technique. The feasibility has been investigated in advance by theoretical analyses. The experimental fiber-optic sensor demonstrates its capability to operate in the aqueous media with the detectable range of refractive indices of 1.33-1.36. A self-assembled monolayer (SAM) of long chain thiol is introduced to cover the surface of silver in order to prevent silver from deterioration. Experimental studies demonstrate that, by this way, the lifetime of sensor increases from some days to some weeks. This work provides a base for developing an affinity biosensor.

Keywords: *Sensor; Surface plasmon; Optical coatings; Sol-gel technique; Self-assembled monolayer (SAM)*

1. Introduction

The fiber-optic based surface plasmon resonance (SPR) sensors have some advantages such as flexibility, low cost, small size and possible use in remote sensing over the traditional bulk optical systems [1]. Recently, a simple SPR multimode fiber-optic sensor using oblique

injection of a parallel monochromatic light has been developed [2,3]. Silver is used to support SPR which is excited by light of 670nm wavelength emitted from a laser diode. However this fiber-optic sensor, with its measurable index range at about 1.35-1.40 [3], is still incapable of monitoring aqueous environment whose refractive index is 1.33-1.36. The limitation has prevented its applications in most practical chemical and biochemical systems.

Two ways can be considered to drop down the range of measurable indices. One is to reduce the wavelength of light source, but the laser diodes commercially available with the wavelength of about 600-900nm do not give much choice. The other solution, as it is adopted in this paper, is to deposit an additional overlay on the surface of the metal film.

Another problem confronted is the deterioration of silver. Gold and silver are known to be the most important metals for SPR applications [4]. Gold is physically and chemically stable while silver can provide the sharpest SPR. But the oxidation of silver happens as soon as exposed to air and especially to water, which gives rise much difficulty to bring about a reliable sensor for practical applications. A treatment of the silver surface by a thin and dense cover is therefore suggested.

The theory in predicting the index-dependent thickness of an overlay is discussed firstly in this paper. A zirconium acetate (marked as ZrO_2 in this paper) overlay is coated on silver surface as thick as some dozen nanometers by sol-gel technique. Lastly, the stability of the fiber-optic sensor is improved by introducing a self-assembled monolayer (SAM) of long chain acid thiol between the layers of silver and ZrO_2 in order to protect the silver film from oxidation.

2. Theory

A relation between the thickness and refractive index of an overlay on four-layer sensor has been studied by W.J.H. Bender et al [5]. As it has been mentioned above, our transducer illustrated in figure 1 is a 5-layer structure that consists of fiber core, metal silver, thiol cover, ZrO_2 overlay and aqueous sample (see in figure 2). Since the thickness in total (less than one hundred nanometers) is rather small compared with its length (15mm) and the diameter of the core (600μm), the sensing section can be treated rather exactly as a one-dimensional multilayered planar configuration.

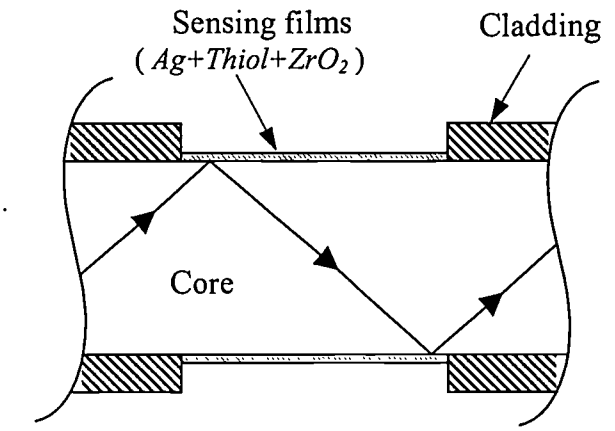

Fig.1. Schematic diagram of fiber-optic sensor

The matrix method for deriving the SPR dispersion relation in a stratified planar structure has been used by number of authors including Born and Wolf [6], Azzam and Bashara [7], Kurosawa et al [8] and Ward et al [9]. Nevertheless part of important derivation is kept in Appendix for some interested readers who could have a complete process and the consistent definitions.

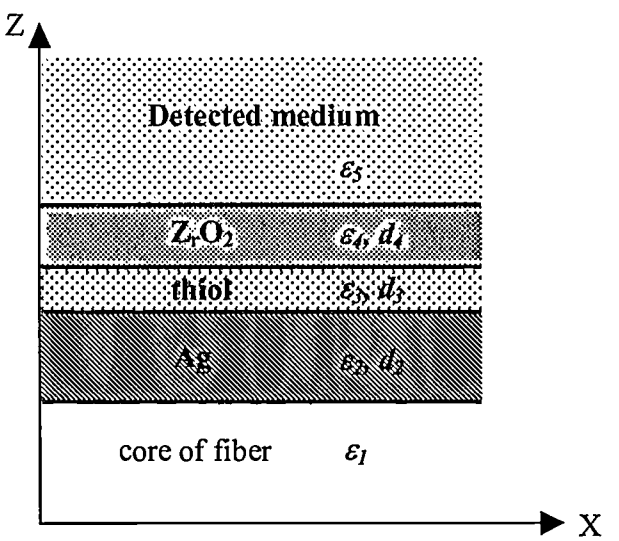

Fig.2. Schematic diagram of our 5-layer configuration

Since the overlay is the 4th layer in our 5-layer system (see figure 2), its thickness is denoted d_4 that can be obtained from the 5-layer SPR dispersion equation $M_{11}(5)=0$ as

$$d_4 = \frac{1}{i2k_{z4}} \ln(-\frac{f_{11}}{g_{11}})$$

where $M_{11}(5)$, k_{z4}, f_{11} and g_{11} are given in expressions (13), (3), (19) and (20) respectively in Appendix.

The refractive index of the surrounding sample is set to be $n_5=1.333$ for the purpose of monitoring the aqueous environment. And the SPR is supposed to be excited by the light rays impacting on the core-metal interface in the fiber with an incident angle between 76.5°-89.5°. This angle range is determined by taking into account the totally internal reflected condition given by its refractive indices of core (1.457) and cladding (1.407) of fiber and the reflected angle distribution of the skew rays propagating through the fiber. Other parameters such as those of silver film (52nm thick with dielectric constant of -19+1.2i at the wavelength of 670nm) and thiol layer (1.77nm thick with refractive index of 1.463) [10] are used in calculations. Since the imaginary part of d_4 (noted as d_{4i}) is very small in contrast to its real part (see figures 3 and 4 obtained for the case of $d_3=0$), the real part of the calculated d_4 is adopted as predicted thickness of the overlay noted as d.

The expression is general and includes the behavioral description of a 4-layer sensor. If the overlay is directly deposited on the silver surface without using a thiol layer, d_3 can be set to zero. The curves plotted in figure 3 show a relation between the thickness and the refractive index of the overlay in the 4-layer system where SPR will be excited by the light rays with the incident angles of 76.5° and 89.5° respectively. The possible values between the two curves of d(76.5°) and d(89.5°) constitute a selectable thickness range for overlay. Since a very thick overlay can be considered as a semi-infinite medium, the very sharp peaks at refractive indices of 1.35 and 1.40 for the curves of d(76.5°) and d(89.5°) respectively indicate a detectable index range of 1.35-1.40 for this kind of fiber-optic SPR sensor while it consists of 3 layers as core/silver/sample. The coherence that this range exactly matches to the result previously reported on the 3-layer sensor [2] proves the reliability of our theoretical analyses.

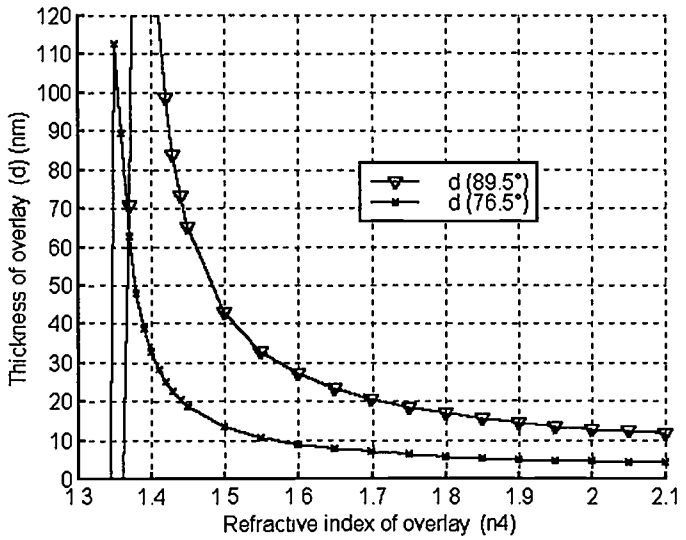

Fig.3 Thickness vs. refractive index of the overlay coated directly on silver surface. The points in the area between d(76.5°)and d(89.5°)give the selectable parameters of overlay. The parameters as n_1=1.457, d_2=52nm, ε_2=-19+1.2i (λ=670nm), d_3=0, n_3=1.463 and n_5=1.333 are used in calculations.

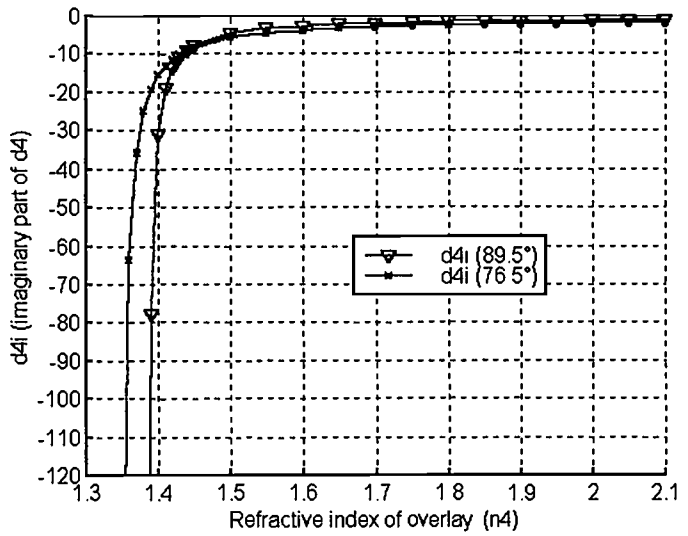

Fig.4 Imaginary part of d_4 vs. refractive index of the overlay coated on silver surface. The parameters as n_1=1.457, d_2=52nm, ε_2=-19+1.2i (λ=670nm), d_3=0, n_3=1.463 and n_5=1.333 are used in calculations.

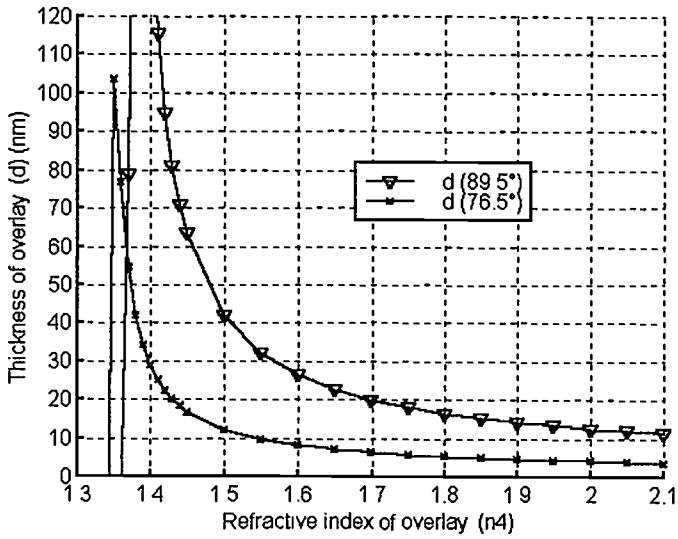

Fig.5 Thickness vs. refractive index of the overlay coated on thiol SAM surface. The points in the area between d(76.5°)and d(89.5°)give the selectable parameters of overlay. The parameters as n_1=1.457, d_2=52nm, ε_2=-19+1.2i (λ=670nm), d_3=1.77nm, n_3=1.463 and n_5=1.333 are used in calculations.

The geometric and material parameters of the overlay in a 5-layer sensor are predicted and the results are plotted in figure 5. There is no much difference between the figures 5 and 3, which can be explained by the fact that the thiol as monomolecular layer is too thin to be important compared to overlay. Moreover, the simulation of this SPR fiber-optic sensor [11] reveals that the sensitivity increases but the dynamic range decreases as the thickness varies from the lower limit to the upper limit. This observation is of significance because the sensitivity and dynamic range of this kind of sensor can be modified to some degree according to the needs of applications.

3. Experiments

3.1 Experimental set-up

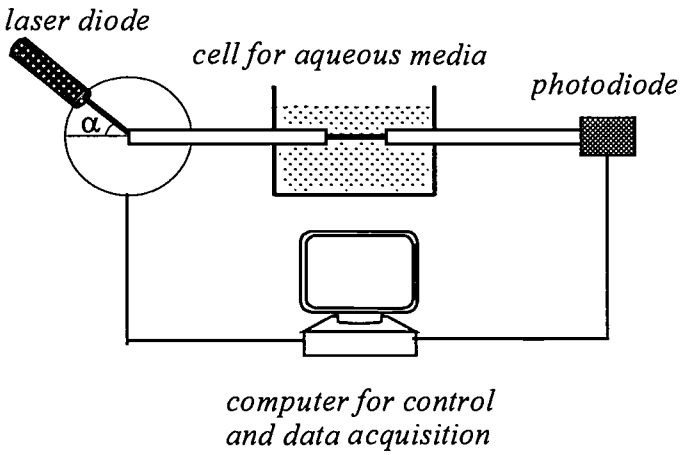

Fig.6. Schematic diagram of the experimental set-up

The measurements were performed on the experimental set-up illustrated in figure 6. The fiber was mounted through a small cell where the sample solutions were contained. The sensor was illuminated by a polarized parallel beam of 670nm wavelength emitted from a collimated laser diode which was installed on a precision rotator. The light power transmitted out of the fiber was completely collected by a photodiode. The photovoltage was amplified, giving a reading proportional to the transmitted light power. All controls and the data-acquisition were automated by using a computer. The tested samples with definite indices monitored by an Abbe refractometer were prepared by diluting ethylene glycol (n=1.4310) with distilled water (n=1.333).

3.2 Deposition of the ZrO_2 overlay by sol-gel

A 15mm length of cladding was removed by mechanical and chemical methods [2,3] from the middle of the 210mm long multimode step-index silica/silicone optical fiber (Quartz et Silice PCS 600). The silver film was deposited on the uncladded part of the fiber core via thermal evaporation. The coating of ZrO_2 overlay was put into effect by sol-gel just after the fiber was taken out of the vacuum chamber.

The input sol was prepared by the mixture of three components: Zirconium(IV) propoxide (70wt% solution in 1-propanol) (Aldrich product), acetic acid and n-propanol (CarloErba products) with the molar ratio of 1:3:95. This composition has been proposed by G.O.Noonan et al [12] but is applied for the first time, as far as we know, to fiber-optic SPR sensing. After the exothermic reaction between acetic acid and Zirconium(IV) propoxide, the mixture was diluted by n-propanol. The metallized fiber was dipped into the input sol for 5 min and then withdrawn with the velocity of 1mm/s. The ZrO_2 overlay was hydrolyzed by air moisture and stabilized on the fiber after heating at 60°C for three hours. Experiments illustrated that the silver film was seriously oxidized if the temperature was raised up to 110°C. The compound formed in these experimental conditions is a metal carboxylate polymer matrix (Zr-O backbone and acetate ligands) and is generally called Zirconium acetate.

The ZrO_2 layer deposited on a Si/SiO_2 substrate was characterized by using ellipsometry. The measured thickness of the ZrO_2 was 18nm with a refractive index of 1.55. These values fell just into the selectable range shown in figure 3.

3.3. Measurements

The performances of this fiber-optic SPR sensor operating as a refractometer were measured in different solutions with definite refractive indices by using the experimental set-up illustrated in figure 1. The output voltage readings were recorded while the laser diode moved, leading to a variation of the external incident angle α from –25° to 25° relative to the axis of fiber. Then the measured data was normalized.

The experimental responses of this sensor before and after the deposition of the ZrO_2 overlay are presented in figure 7(1) and 7(2). The comparison of these two figures clearly indicates that the measurable index range has been successfully drawn down as the theory has predicted.

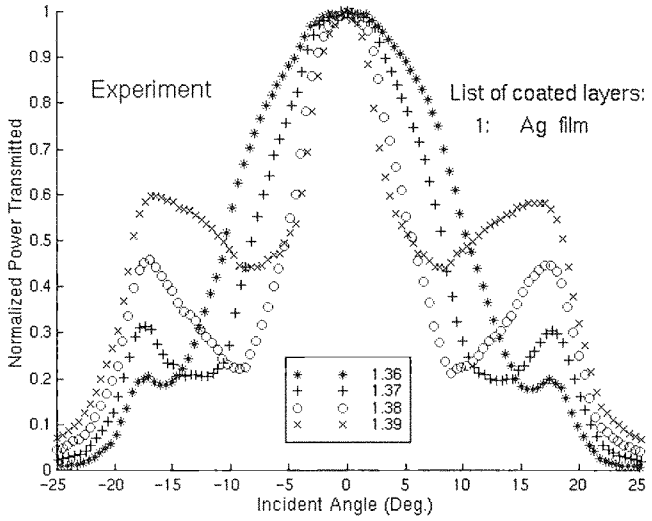

Fig.7(1) Measurements in the solutions with the refractive indices of 1.36, 1.37, 1.38 and 1.39 respectively for the sensor before the deposition of ZrO_2

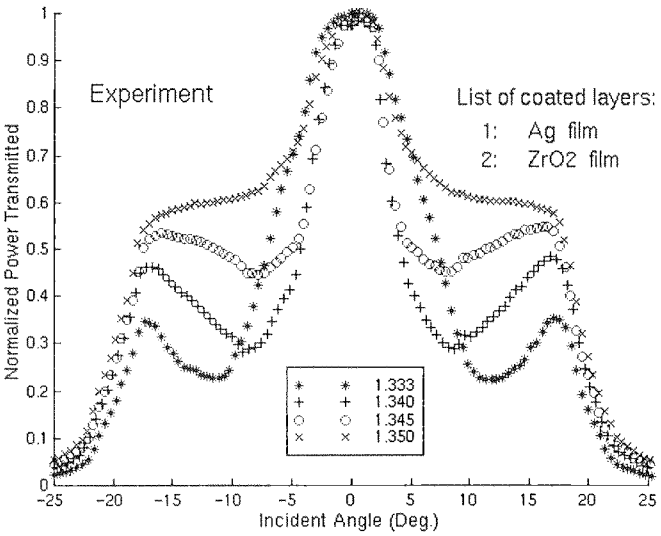

Fig.7(2) Measurements in the solutions with the refractive indices of 1.333, 1.340, 1.345 and 1.350 respectively for the sensor after the deposition of ZrO_2

3.4. Experimental studies on reliability

Unfortunately, the performances of this sensor deteriorated in a few days while exposed to air. The evolution was characterized in figure 8 by measuring the SPR responses in aqueous solutions with definite refractive indices of 1.33, 1.345, 1.350, 1.355 respectively on the 2^{nd} and 12^{th} days.

It's obvious that the overlay of ZrO_2 was not dense enough to protect the silver from oxidation. Therefore, the acid thiols with both long chain (11 Mercaptoundecanoic acid, synthesized at IBCP-CNRS Lyon) and short chain (Mercaptoacetic acid, Sigma product) were introduced to further experiments. Prior to the elaboration of the ZrO_2 layer, the metallized fibers were dipped into the thiol solutions at 10^{-3} M concentration for 2 hours in order to constitute a self-assembled monolayer (SAM) of thiol on the silver surface. The experimental results demonstrate that the thiol can ameliorate the lifetime of the sensor as well as its mechanical strength. Moreover, the sensor using the long chain acid thiol is much more stable than that using short chain one. This phenomenon can be explained as that the long chain thiol is able to build a monolayer much denser than the short chain thiol. The evolutions shown in figure 9 for an experimental sensor with long chain acid thiol, which is conserved in air and measured in pure water on the 4^{th}, 21^{st}, 40^{th} and 70^{th} days respectively, demonstrate that this sensor can keep its function reliable for about three weeks. A remarkable improvement, from some days to some weeks for the lifetime of the SPR sensor using silver, demonstrates the value of this work. This chemical treatment to the silver surface using a thiol SAM can be applied to other SPR devices such as the traditional prism-based systems while silver is used.

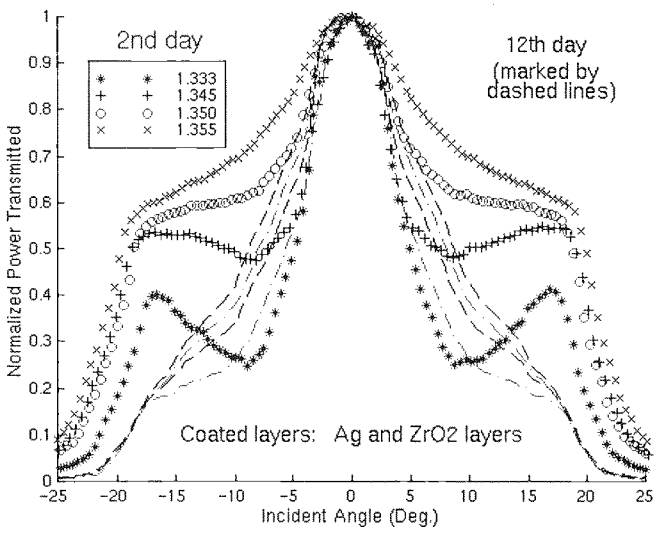

Fig.8 Evolution of an experimental sensor without thiol where the sensor is conserved in air and the measurements are carried out in aqueous solutions with the refractive indices of 1.33, 1.345, 1.350, 1.355 respectively on the 2^{nd} and 12^{th} days.

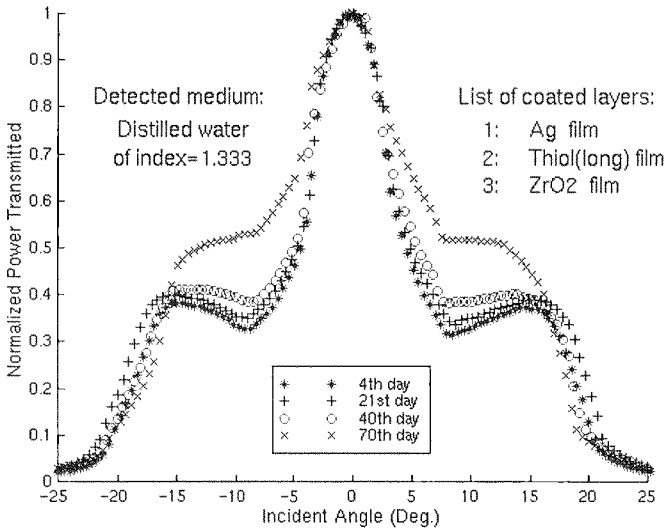

Fig.9 Evolution of an experimental sensor with the long chain thiol acid, where the sensor is conserved in air and the measurements are carried out in pure water on the 4^{th}, 21^{st}, 40^{th} and 70^{th} days respectively.

4. Conclusions

Two thin films of ZrO_2 and thiol are successfully introduced into the structure of the SPR fiber-optic sensor formerly developed to improve its performances in order to be able to apply for chemical and biological sensing. The selectable thickness and refractive index of an overlay are predicted by theoretical analyses. A new material of ZrO_2 is used to the fiber-optic SPR sensors. The sol-gel technique is proven to be an effective means to coat a uniform thin film with very good repeatability. The experimental researches of stability are important as well because the deterioration of silver film is always a serious problem for the SPR sensors using silver. Our work has illustrated a feasible way to realize a practical SPR fiber-optic sensor that is capable of monitoring aqueous medium. Furthermore a SPR fiber-optic affinity biosensor can be anticipated based on this system.

Appendix

A stratified structure is illustrated in Figure A1. The co-ordinate system is chosen so that the layers are stacked along the z-axis and have infinite extent in x and y direction. The arbitrary medium layer j is defined by the thickness d_j and dielectric constant ε_j. The layers 1 and n are both semi-infinite media which in our case are the core of the fiber and the measured surrounding medium respectively. All the dielectrics and metal are considered uniform and isotropic.

$\boldsymbol{A}(A_x,A_y,A_z)$ and $\boldsymbol{B}(B_x,B_y,B_z)$ are the electric field vectors with their components in three directions for the forward and backward plane waves respectively. The positive directions of these components are defined as well in Fig.A1.

The p-polarised incident monochromatic plane wave is at first considered. The Maxwell's equations are solved in omitting the common factors of $exp[i(k_x x-\omega t)]$ and the fields in the layer j can be written as[4]

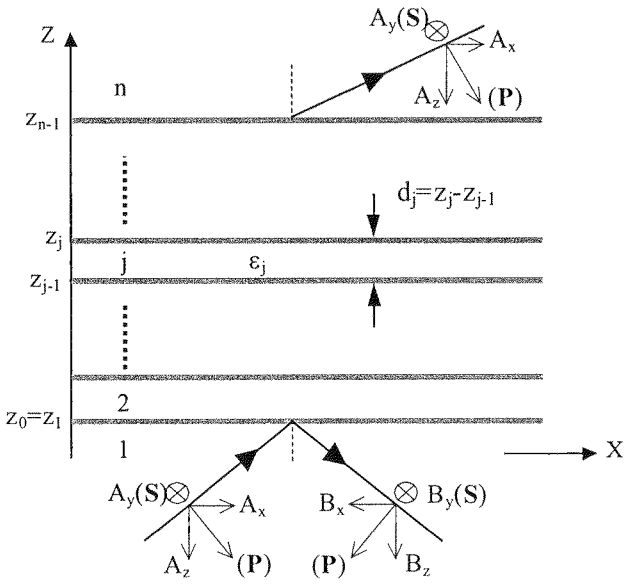

Fig.A1. Schematic diagram of n-layer stratified configuration

$$\mathbf{E}_j=A_{xj}\,exp[i\,k_{zj}\,(z-z_{j-1})]\;(1,0,-k_x/k_{zj})-B_{xj}\,exp[-i\,k_{zj}\,(z-z_{j-1})]\;(1,0,\,k_x/k_{zj}) \quad (1)$$

$$\mathbf{H}_j=k_0 A_{xj}exp[i\,k_{zj}\,(z-z_{j-1})]\;(0,\,k_x/k_{zj},0)+k_0\,B_{xj}\,exp[-i\,k_{zj}\,(z-z_{j-1})]\;(0,\,k_x/k_{zj},0) \quad (2)$$

where $k_0=2\pi/\lambda$ and

$$k_{zj}=[k_0{}^2\varepsilon_j - k_x{}^2]^{1/2} \quad (3)$$

where λ is the light wavelength and k_0 is the amplitude of wave vector in vacuum. k_z and $k_x = k_0\,n_1\sin\psi$ are wave vector components in media along the z and x directions respectively, here ψ is the angle of incidence.

By applying the boundary conditions at $z=z_j$ interface, the relation between the parameters in the layers of j and $j+1$ can be obtained

$$\begin{bmatrix} A_{xj} \\ B_{xj} \end{bmatrix} = \frac{1}{2\alpha_j\,\beta_k{}^{\frac{1}{2}}} M(j,j+1) \begin{bmatrix} A_{xj+1} \\ B_{xj+1} \end{bmatrix} \quad (4)$$

where $M(j,j+1)$ is a matrix

$$M(j,j+1) = \begin{bmatrix} \alpha_{j+1}+\alpha_j & \alpha_{j+1}-\alpha_j \\ (\alpha_{j+1}-\alpha_j)\beta_j & (\alpha_{j+1}+\alpha_j)\beta_j \end{bmatrix} \quad (5)$$

here

$$\alpha_j=\varepsilon_j/k_{zj} \quad (6)$$

$$\beta_j = exp(i2k_{zj}\, d_j) \tag{7}$$

By repeating the relation expressed in (4) in different layers, we have

$$\begin{bmatrix} A_{x1} \\ B_{x1} \end{bmatrix} = \frac{1}{2^{n-1} \prod_{k=1}^{n-1} (\alpha_{k+1}\, \beta_k \frac{1}{2})} \begin{bmatrix} M_{11}(n) & M_{12}(n) \\ M_{21}(n) & M_{22}(n) \end{bmatrix} \begin{bmatrix} A_{xn} \\ B_{xn} \end{bmatrix} \tag{8}$$

Therefore, the dispersion equation is acquired as [8,13]

$$M_{11}(n) = 0 \tag{9}$$

The amplitude reflectivity is defined as the complex amplitude ratio of the reflected wave to the incident wave. The amplitude reflectivity for p-polarised incident light r_p is yielded as

$$r_p = M_{21}(n)/M_{11}(n) \tag{10}$$

For s-polarization, we have proven that all results in this paper can keep the same expressions if $\alpha_j = \varepsilon_j / k_{zj}$ in equation (6) is substituted by

$$\alpha_j = k_{zj} \tag{11}$$

except the amplitude reflectivity for s-polarised incidence that should be

$$r_s = -\, M_{21}(n)/M_{11}(n) \tag{12}$$

It is well known that in non-magnetic media SPR could only exist for p-polarization of electromagnetic fields [14]. The M_{11} and M_{21} for p-polarization plane wave incident in the 5-layered geometry (see figure 2 as an example) can be derived after much of algebra as

$$M_{11}(5) = f_{11} + g_{11}\, \beta_4 \tag{13}$$

$$M_{21}(5) = f_{21} + g_{21}\, \beta_4 \tag{14}$$

where

$$c_1 = (\alpha_2+\alpha_1)(\alpha_3+\alpha_2) + (\alpha_2-\alpha_1)(\alpha_3-\alpha_2)\, \beta_2 \tag{15}$$

$$c_2 = (\alpha_2+\alpha_1)(\alpha_3-\alpha_2) + (\alpha_2-\alpha_1)(\alpha_3+\alpha_2)\, \beta_2 \tag{16}$$

$$c_3 = (\alpha_2-\alpha_1)(\alpha_3+\alpha_2) + (\alpha_2+\alpha_1)(\alpha_3-\alpha_2)\, \beta_2 \tag{17}$$

$$c_4 = (\alpha_2-\alpha_1)(\alpha_3-\alpha_2) + (\alpha_2+\alpha_1)(\alpha_3+\alpha_2)\, \beta_2 \tag{18}$$

$$f_{11} = (\alpha_5+\alpha_4)[(\alpha_4+\alpha_3)\, c_1 + (\alpha_4-\alpha_3)\, c_2\beta_3] \tag{19}$$

$$g_{11} = (\alpha_5-\alpha_4)[(\alpha_4-\alpha_3)\, c_1 + (\alpha_4+\alpha_3)\, c_2\beta_3] \tag{20}$$

$$f_{21} = (\alpha_5+\alpha_4)[(\alpha_4+\alpha_3)\, c_3 + (\alpha_4-\alpha_3)\, c_4\beta_3] \tag{21}$$

$$g_{21} = (\alpha_5-\alpha_4)[(\alpha_4-\alpha_3)\, c_3 + (\alpha_4+\alpha_3)\, c_4\beta_3] \tag{22}$$

The derivation can be verified by setting $\varepsilon_2 = \varepsilon_3 = \varepsilon_4 = \varepsilon_5$ (*i.e.* $\alpha_2 = \alpha_3 = \alpha_4 = \alpha_5$) in $M_{11}(5) = 0$ in the case of p-polarisation. The well-known relation of SPR for one boundary geometry can be consequently yielded [15]

$$k_x = k_0 \left(\frac{\varepsilon_1 \varepsilon_2}{\varepsilon_1 + \varepsilon_2}\right)^{1/2} \quad (23)$$

References

1. R.C.Jorgenson and S.S. Yee, A fiber-optic chemical sensor based on surface plasmon resonance, Sensors and Actuators B, 12(1993) 213-220

2. C.Ronot-Trioli, A.Trouillet, C.Veillas A.El-Shaikh and H.Gagnaire, Fibre optic chemical sensor based on surface plasmon monochromatic excitation, Analytica Chimica Acta 319(1996) 121-127

3. A Trouillet, C.Ronot-Trioli, C.Veillas and H.Gagnaire, Chemical sensing by surface plasmon resonance in a multimode optical fibre, Pure Appl. Opt. 5(1996) 227-237

4. G. Kovacs, Optical excitation of surface plasmon-polaritons in layered media, Electromagnetic Surface Modes, Edited by A.D. Boardman, 1982 John Wiley & Sons Ltd. p.143-200

5. W.J.H.Bender, R.E.Dessy, M.S.Miller and R.O.Claus, Feasibility of a chemical microsensor based on surface plasmon resonance on fiber optics modified by multilayer vapor deposition, Anal. Chem. 66(1994) 963-970

6. M.Bron and E.Wolf, Principles of Optics, Third (revised) edition, Pergamon Press

7. R.M.A.AZZAM and N.M.BASHARA, Ellipsometry and polarized light, North-Holland Publishing Company (1977) p.332-340

8. K. Kurosawa, R.M.Pierre , S.Ushioda, J.C.Hemminger, Raman scattering and attenuated-total reflection studies of surface-plasmon polariton, Phys. Rev. B, 33(1986) 789-798

9. C.A.Ward, K.Bhasin, R.J.Bell, R.W.Alexander and I.Tyler, Multimedia dispersion relation for surface electromagnetic waves, J. Chem. Phys., 62(1975) 1674-1676

10. D.R Lide, Handbook of Chemistry Physics, 71st ed.(1990), CRC Press

11. W.B.Lin, N.Jaffrezic-Renault, A.Gagnaire, H.Gagnaire, The Effects of Polarization of the Incident Light -- Modeling and Analysis of a SPR Multimode Optical Fiber Sensor, Sens. Actuators A, In press

12. G.O.Noonan and J.S.Ledford, Structure and chemical sensing applications of zirconium acetate sol-gel films, Chem.Mater. 7(1995) 1117-1123

13. I.Pockrand, Surface plasmon oscillations at silver surfaces with thin transparent and absorbing coatings, Surface Science 72(1978) 577-588

14. K.L.Kliewer and R.Fuchs, Collective electronic motion in a metallic slab, Phys. Rev., 153(1967) 498-512

15. J.R. Sambles, G.W. Bradrery and Fuzi YANG, Optical excitation of surface plasmons: an introduction, Contemp. Phys., 32(1991) 173-183

Les effets de la polarisation de la lumière incidente —Modélisation et analyse d'un capteur SPR à fibre multimodale

Résumé Article 2

Les effets de la polarisation de la lumière incidente –Modélisation et analyse d'un capteur SPR à fibre multimodale

Il est bien connu que la résonance de plasmon de surface ne peut être excitée que par la polarisation p de la lumière. D'autre part, le phénomène de mélange de mode lors de la propagation des rayons le long d'une fibre optique multimodale est connu depuis longtemps. Quel effet est le plus important pour le capteur SPR à fibre optique multimodale ?

Notre capteur devant détecter de très faibles variations d'un paramètre à suivre, un modèle théorique le plus précis possible doit être établi. Les influences de la polarisation de la lumière incidente par rapport à la face d'entrée de la fibre sur la réponse d'un capteur SPR à fibre optique seront étudiées dans cet article.

Nous sommes partis de la conclusion [1] que l'énergie lumineuse transmise dans un capteur à fibre optique n'est pas influencée par la direction de polarisation de la lumière incidente et nous avons obtenu des résultats expérimentaux qui montrent des différences apparentes de la puissance lumineuse normalisée transmise pour des illuminations par une polarisation p ou s de la lumière. Donc un modèle 3D précis, basé sur l'optique géométrique, a été développé, dans lequel on étudie les variations spatiales du vecteur champ électrique lors de la propagation des rayons non-méridiens dans la fibre multimodale. Les calculs sont en bon accord avec les expériences. Des études plus approfondies ont permis de tirer les conclusions suivantes :

- La polarisation de la lumière incidente a d'autant plus d'influence que la partie SPR est située plus près de la face d'entrée de la fibre.
- La polarisation de la source de lumière n'a pas beaucoup d'influence si la partie SPR se trouve loin de la face d'entrée de la fibre. Dans ce cas, on retombe sur la conclusion de la référence [1].
- Cependant, le modèle précis est intéressant à utiliser pour traiter des faibles signaux provenant du capteur.

Ce travail non seulement permet de clarifier les concepts fondamentaux mais aussi rend possible la caractérisation d'un film métallique, d'une monocouche d'alkylthiol auto-assemblée et de couches anticorps-antigène, comme le montre les articles suivants.

Références :1. C.Ronot-Trioli, A.Trouillet, C.Veillas, A.El-Shaikh and H.Gagnaire, Fibre optic chemical sensor based on surface plasmon monochromatic excitation, Analytica Chimica Acta, 319(1996) 121-127

Preface to article 2

The Effects of Polarization of the Incident Light --- Modeling and Analysis of a SPR Multimode Optical Fiber Sensor

It is well know that the SPR can only be excited by p-polarized light. In the other hand, the phenomenon of the mode mixture as the light rays propagate through a multimode optical fiber has been recognized for a long time. Then which effect is more important in the SPR multimode fiber-optic sensor? Since our sensor is aimed to detect the slight variations of a monitored parameter and moreover to interpret the small signals, a theoretical model as precise as possible is expected. The influences of the polarization of incident light with respect to the input end face of the fiber to a multimode SPR fiber-optic sensor will be answered in this paper.

We start with the earlier conclusion[1] declared that the light energy transmitted out of the fiber-optic sensor is not affected by the polarization direction of the incident light, and show the experimental results who indicate the apparent differences of the normalized light power transmitted out of the fiber between the illuminations of p- and s- polarized light. Then an accurate 3D model based on geometric optics is developed where the spatial variations of the electric field vector during the propagation of the skew rays in the multimode fiber are investigated. The computations are in good agreements with the experiments. Further studies have drawn out the conclusions as below:

- The polarization of the incident light has much influence while the SPR transducer is located near to the input end of the fiber.
- The polarization of the light source has not much influence while the SPR transducer is far from the input end of the fiber. Therefore, a consistent explanation to the previous conclusion[1] is reached.
- Nevertheless, the accurate model is proposed to use if the small sensing signals need to be quantitatively interpreted.

This research not only clarifies the fundamental concepts but also makes possible to characterize the metal film, the self-assembled alkylthiol monolayer and the antibody and antigen layers demonstrated in the following articles.

References

1. C.Ronot-Trioli, A.Trouillet, C.Veillas, A.El-Shaikh and H.Gagnaire, Fibre optic chemical sensor based on surface plasmon monochromatic excitation, Analytica Chimica Acta, 319(1996) 121-127

The Effects of Polarization of the Incident Light --- Modeling and Analysis of a SPR Multimode Optical Fiber Sensor

Wen Bin LIN[a,d], Nicole JAFFREZIC-RENAULT[a,*], Alain GAGNAIRE[b], Henri GAGNAIRE[c]

[a] IFOS / [b] LEOM , Ecole Centrale de Lyon, 36 Avenue Guy de Collongue, BP163, 69131 Ecully Cedex, France

[c] TSI, Université Jean Monnet, 23 Rue du Dr. Paul Michelon, 42023 Saint-Etienne Cedex, France

[d] Electronic Science Department, Nankai University, Tianjin, 30071, China

[*] ***Corresponding author:*** *Tel: +33 4 72186243; Fax: +33 4 78331577; Email: Nicole.Jaffrezic@ec-lyon.fr*

Abstract: A 3D skew ray modeling has been developed to consistently explain the experimental phenomena for an intrinsic SPR multimode optical fiber sensor. The effects of the polarization direction of the incident light at certain conditions have been clarified. This simulation is needed to accurately detect the variations of the refractive index of the bulk medium and of the thickness of the thin surface layer. More complete knowledge about light energy transmission by the skew ray in the multimode step-index fiber is obtained by this investigation.

Keywords: *Fiber-optic sensor; Surface plasmon resonance; Simulation; Polarization effect; Accurate detection*

1. Introduction

An intrinsic multimode fiber-optic sensor based on surface plasmon resonance (SPR) has been previously reported[1-4]. The transducer uses a multimode optical fiber whose cladding is modified by the multilayered thin films including a metallic layer deposited on the fiber core and is illuminated by a collimated oblique monochromatic light emitted from a laser diode. This approach is simpler and cheaper than some other fiber-optic arrangements such as that of R.C.Jorgenson and S.S.Yee[5] and commercially available BIACORE (Sweden). The possible portability makes it attractive to domicile applications for medical, food and environmental analysis.

Earlier studies[3] have concluded that the light energy transmitted out of the fiber-optic is not affected by the polarization of the incident light. This phenomenon can be explained by mode mixing in multimode optical fiber. The modeling based on geometric optics was then developed[4].

We show in this paper the existence of the influences of the polarization of the incident light. Moreover, in certain conditions, these influences are important. We begin with the experimental results that demonstrate the apparent differences of the normalized light power transmitted out of the fiber between the illuminations of p- and s- polarized light. The measured fiber is only 10cm long that is applicable to the future portable device. A 3D model that resolves the electric field into p- and s- components during the light propagation has been developed. The computations agree well with the experiments. The next part of this paper is devoted to investigate the influences of the p- and s- polarized incident light to the transmitted light power and the sensitivity of the sensor. The conditions at which this 3D model has to be used are concluded. The validity and limit of the earlier conclusions[3] are clarified.

2. Experiments

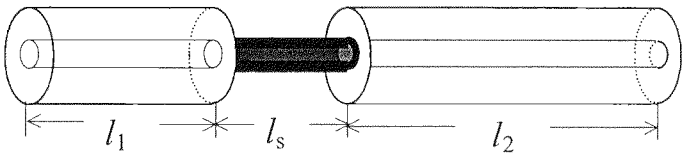

Fig.1. Schematic representation of the fiber-optic sensor

The fiber optic used in our experiments was the multimode step-index silica/silicone optical fiber (Quartz et Silice PCS 600). A total length of 100mm fiber was cut and its two ends were carefully polished to minimize the scattering of light. A section of cladding from 4mm to 19mm was removed by mechanical and chemical methods[1-3]. Then a gold film of 55nm thick, monitored by a quartz-crystal detector, was deposited on this section via thermal evaporation. After 2 days for stabilization of the metal film exposed to air at room temperature, the fiber (see figure 1) was mounted through a small cell which contained the tested solutions with certain indices monitored by an Abbe refractometer. The mixture of

distilled water (n=1.333 /20°C) and ethylene glycol (n=1.4310 /20°C) provided the tested solutions with different indices by varying the proportions of the two compositions.

The measurements were performed on the experimental set-up illustrated in figure 2. The sensor is illuminated by a polarized parallel beam of 670nm wavelength emitted from a collimated laser diode which is installed on a precision rotator. The light power transmitted out of the fiber is completely collected by a photodiode. All controls and the data-acquisition are automated by using a computer.

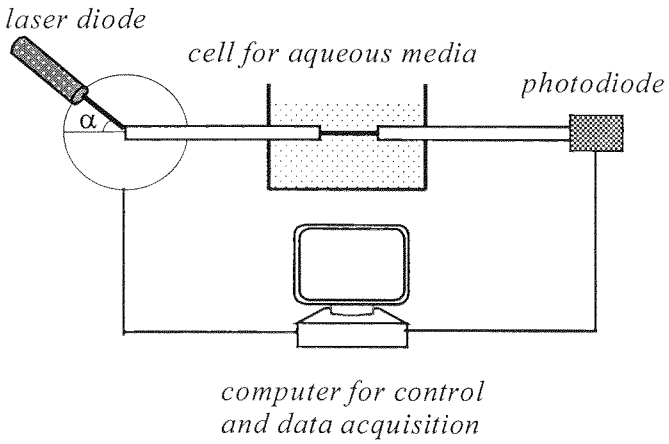

Fig.2. Schematic representation of the experimental set-up

The responses of the sensor with both p- and s- polarized illuminations were recorded. The different effects between p- and s- polarization of incident light are clearly revealed by the experiments demonstrated in figure 3.

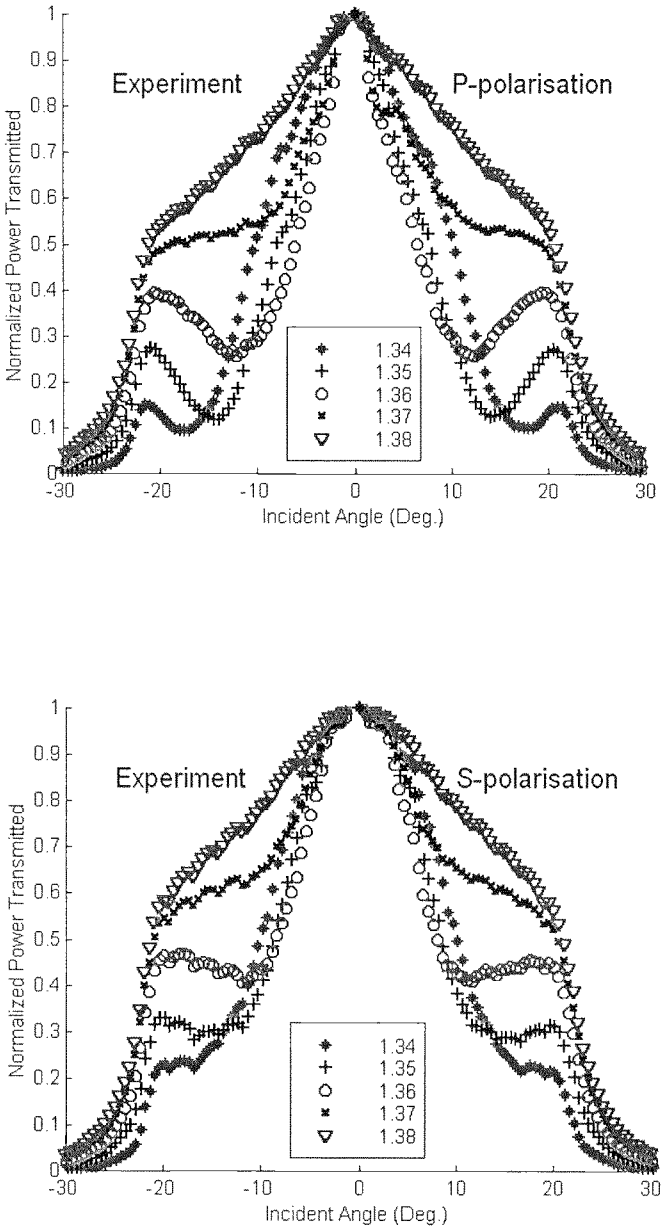

Fig.3 Experimental curves of the normalized light power transmitted vs. incident angle by incident light of p- and s- polarization (l_1=4mm, l_s=15mm and l_2=81mm; thickness of gold film=55nm; indices of measured bulk media=1.34, 1.35, 1.36, 1.37 and 1.38 respectively)

3. Theoretical model

3.1 Introduction

It is known that the size of core (ϕ=600μm) is so large compared with the optical wavelength (λ=670nm) that the light propagation can be handled almost exactly using geometrical optics. Nevertheless, the study in skew rays is rather complex; authors often restricted the analysis to the case of meridional rays[5,6]. Some papers dealt with skew rays[4,7], but the variation of the direction of the electric field vector at each internal reflection along the ray propagation has not been taken into account.

Surface plasmon resonance (SPR) is a resonance phenomenon occurring at metal-dielectric interface. Under certain conditions, most of the incident light energy can be transferred to the evanescent surface waves resulting in a dramatic attenuation of the reflected light intensity. However, in non-magnetic media, evanescent surface waves could only exist for p-polarization of electromagnetic fields[8] which causes an obvious change at each reflection of the electric field vector direction determined by the amplitude ratio of its p- and s-components.

Hence, it is reasonable to believe that the SPR sensing transducer, which takes place of a section of fiber cladding, would affect the light power transmission in the multimode optical fiber and make the effects of the p- and s- polarized illuminations be distinguishable.

3.2. Brief review of the skew ray trajectory

A general skew ray undergoing into the fiber between two successive reflections is illustrated in figure 4. It has been known that the internal reflection angle Ψ can be yielded from the equation[4,7]:

$$\cos\Psi = \mathbf{u}\cdot\mathbf{n} = \sin\theta\cdot\cos\beta \qquad (1)$$

and that the process between two successive reflections will repeat in the same way as the coordinates correspondingly rotate in XY plane after each internal reflection by the angle of π-2β in the clockwise sense. The projection drawing of the skew trajectory on the input end of the fiber can be depicted in figure 5 with |BC|=|CD|=|DE|=....[9]. So the analyses to the resolution of electric field vector along the light propagation can be focused to one part of the light ray between two successive reflections.

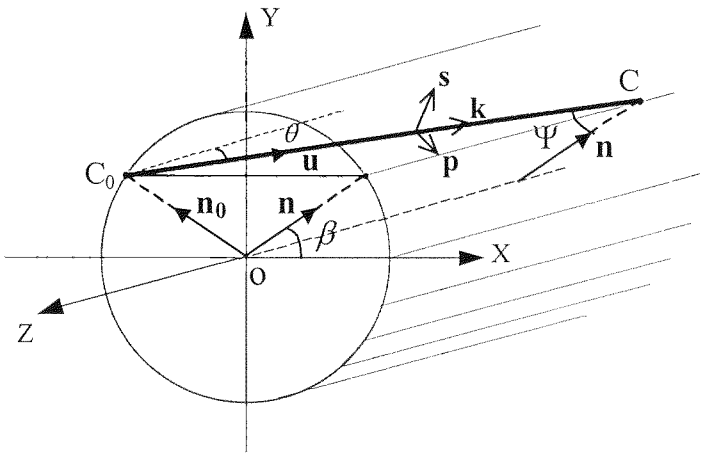

Fig.4 Skew ray propagation and the direction variation of electric field vector in the multimode fiber between two successive reflections

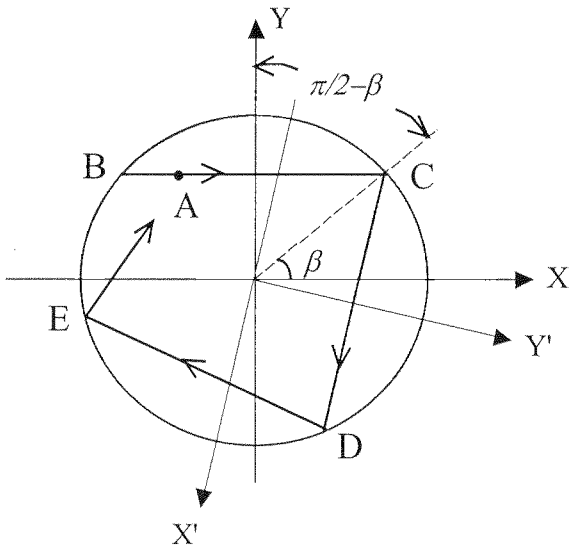

Fig.5 Projection drawing of the skew trajectory on the input end of the fiber

3.3. Decomposition of Electric field

The electric field vector perpendicular to the direction of propagation can be decomposed, according to the plane of incidence, into p-polarized (parallel to the plane of incidence) and s-polarized (orthogonal to the plane of incidence) denoted by **P** and **S** respectively. Considering that **s**, the unit vector of **S**, can be set to keep its direction after the reflection[10], a dynamic local rectangular coordinates defined by the unit vectors **p, s** and **k** (wave vector, in the direction of propagation) as **p** x **s** = **k**, is constituted along the trajectory of skew ray to evaluate the variation of **s** direction in two successive reflections (see figure 4).

Assuming that the s-components of electric field for the light rays input and output of the fiber are in Y direction defined by the unit vector of **y**, and that the two successive reflections take place at point Co and C respectively, the unit vectors of s-component of electric field at points Co designated as $\mathbf{s}_o$ and C designated as **s** can be obtained by

$$\mathbf{s}_o = \mathbf{u} \times \mathbf{n}_o \tag{2}$$

and

$$\mathbf{s} = \mathbf{u} \times \mathbf{n} \tag{3}$$

where **u** is the direction vector of the ray CoC as

$$\mathbf{u} = \mathbf{x}\cdot\sin\theta - \mathbf{z}\cdot\cos\theta \tag{4}$$

and $\mathbf{n}_o$ and **n** are the unit vectors normal to the reflection interface at points Co and C respectively

$$\mathbf{n}_o = -\mathbf{x}\cdot\cos\beta + \mathbf{y}\cdot\sin\beta \tag{5}$$

$$\mathbf{n} = \mathbf{x}\cdot\cos\beta + \mathbf{y}\cdot\sin\beta \tag{6}$$

It can be proven that if $\mathbf{s}_o$ rotates around the axis of wave vector **k** in the clockwise sense by the angle of ω:

$$\omega = \cos^{-1}(\sin\beta / \sin\psi) \tag{7}$$

it reaches to **y**, and the same thing happens from **y** to **s**.

Hence, it can be concluded that the total rotation of the s-polarized vector between two reflections is 2ω in clockwise sense in the dynamic local rectangular coordinates constituted by the unit vectors of **p, s** and **k**.

3.4 Numerical results

Since the gold layer thickness (55nm) is rather small compared with its length (15mm) and the diameter of the core (600μm), the sensing section can be treated as one dimension

multilayered planar structure. Both of the reflectivity to the p- and s- polarized electric field components in this configuration can be calculated by matrix method[11].

The programs written in Matlab have been developed. The computed results for the measured fiber are illustrated in figure 6 by utilizing the parameters: the dielectric constant of 55nm gold film is -13.8+i 1.8 at wavelength of 670nm, the refractive index of core and cladding are 1.457 and 1.407+i 5.4406×10^{-5} respectively at the room temperature. The imaginary part of the index of the cladding is previously determined by the least-square fit of the experimental curve measured in air for the same fiber prior to the deposition of gold layer. The computational curves agree well with the experimental ones (cf. figure 3).

4. Analysis of the fiber-optic sensor

4.1 Sensitivity

This kind of fiber-optic sensor usually works with a fixed incident angle to monitor the variation of the detected parameter such as the refractive index of the bulk medium by measuring the change of the transmitted light power. Figure 7 illustrated both the theoretical and experimental responses of the measured fiber in p- and s- polarized illumination at some fixed incident angles of 8°, 12° 16° and 20° respectively. The good agreements between the computations and the experiments prove the validity of this 3D model.

The sensitivity of the sensor in monitoring the refractive indices of the bulk media is defined as the derivative of the normalized light power transmitted with respect to refractive index. Correspondingly, the curves of sensitivity for p- and s- polarization of incident light respectively are calculated and plotted in figure 8. They demonstrate that the p-polarization illumination has higher sensitivity than s-polarization. It is evident because only p-polarized component of the electric-field serves to the SPR sensing. However, the sensitivity between p- and s- polarization illuminations becomes hard to be distinguished as the SPR sensing part is far away from the input end of the fiber. An example is given in figure 9 for l_1, the distance from the input end of the fiber to the SPR sensing part, is equal to 80mm, as other parameters in these calculations are kept constant.

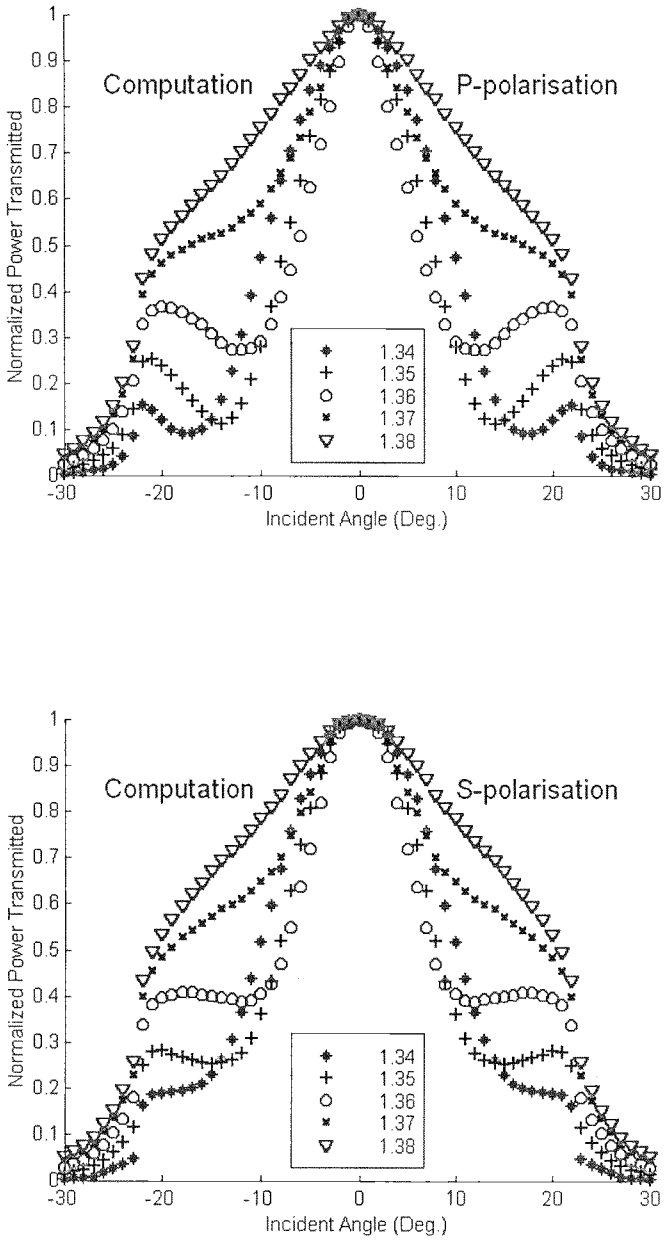

Fig.6 Theoretical curves of the normalized light power transmitted vs. angle of incidence for p- and s- polarization of the incident light (l_1=4mm, l_s=15mm and l_2=81mm; thickness of gold film=55nm; indices of monitored bulk media=1.34, 1.35, 1.36, 1.37 and 1.38 respectively)

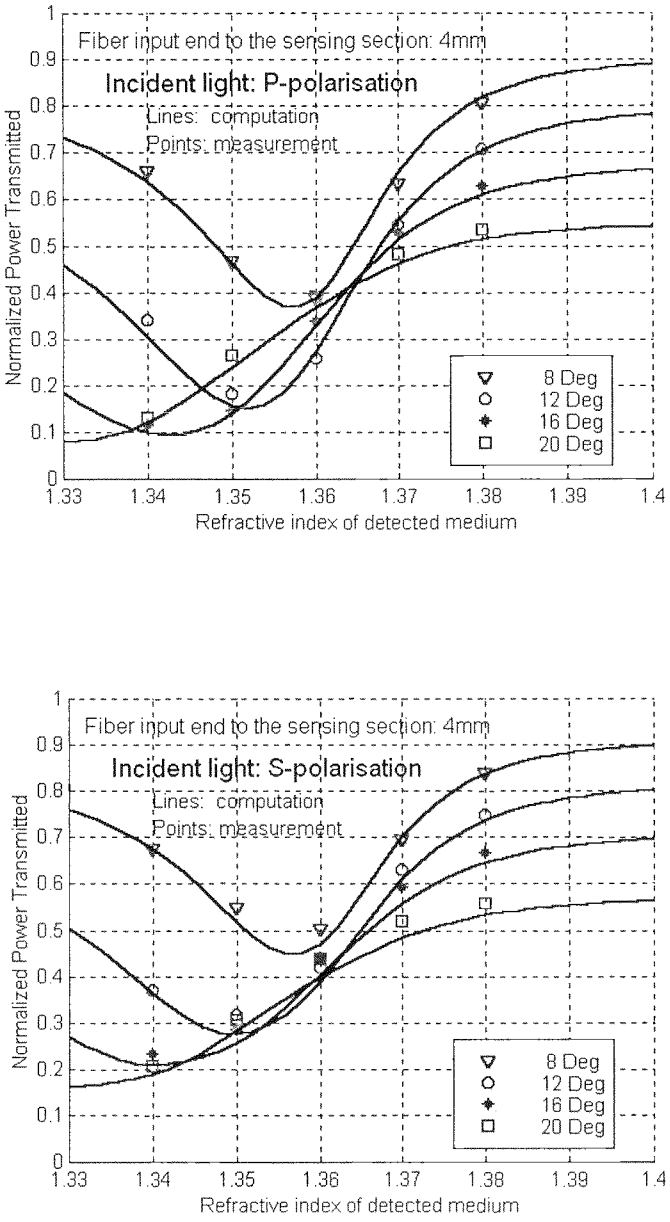

Fig.7 Experimental and theoretical responses at the incident angles of 8°, 12°, 16° and 20° and by p- and s-polarized illuminations respectively vs. the indices of monitored bulk media (l_1=4mm, l_s=15mm and l_2=81mm; thickness of gold film=55nm)

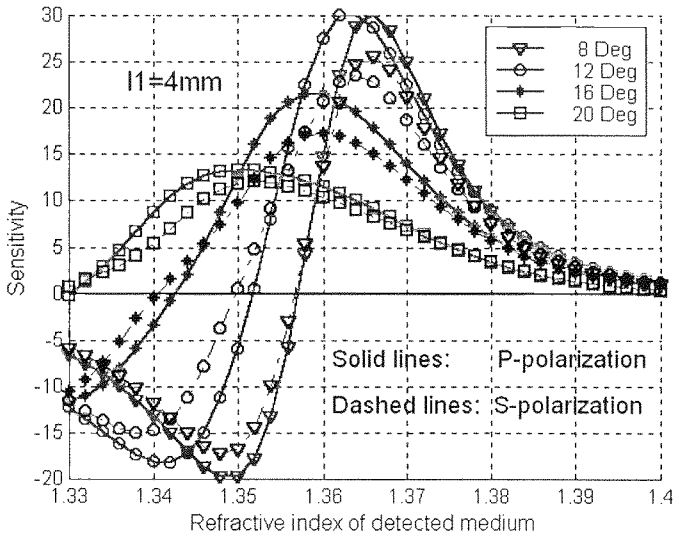

Fig.8 Computed sensitivity with l_1=4mm (l_s=15mm and l_2=81mm, thickness of gold film=55nm)

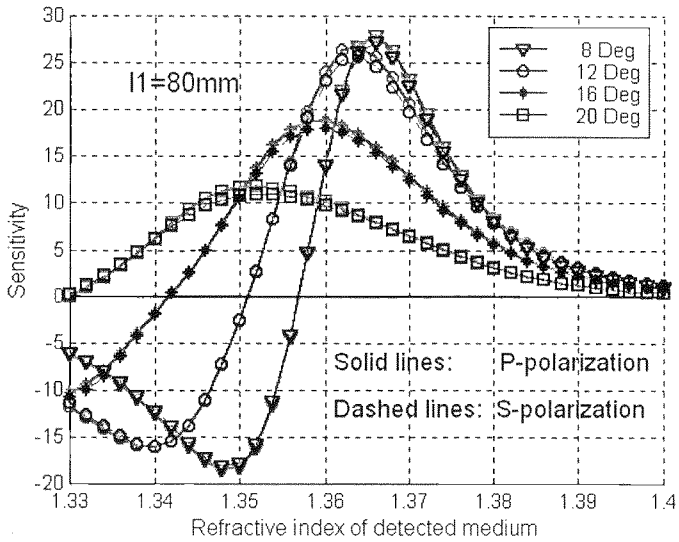

Fig.9 Computed sensitivity with l_1=80mm (l_s=15mm and l_2=81mm, thickness of gold film=55nm)

4.2 Effects of polarization of incident light

Attention is next turned to study the conditions at which the influences of electric field polarization of the incident light can be negligible or reversely need to be taken into account. Assuming that the SPR sensing part keeps the same distance to the output end of the fiber, i.e. l_2=81mm (cf. fig.1), we deal with the differences of normalized light power curves between p- and s- polarized illuminations and see how they vary with l_1. The maximal difference of these two curves is evaluated between the incident angles of 5° and 20° where the influences of p- and s- polarization are most important. Furthermore the maximal difference as a function of l_1 is calculated and the four curves correspondent to four monitored environments with the indices of 1.34, 1.35, 1.36 and 1.37 respectively are plotted in figure 10. The corrugations in the curves come from the spiral way of the light propagation in the multimode optical fiber described in Section **3.2**. It makes clear that while l_1 is greater than 16mm, the influences of polarization illuminations are rather small. The maximum of the four curves at l_1 >16mm is only about 0.02. If it can be considered negligible, the responses of the sensors will show identical to whatever polarization of the incident light. The earlier experimental results[3] can be well explained in this case.

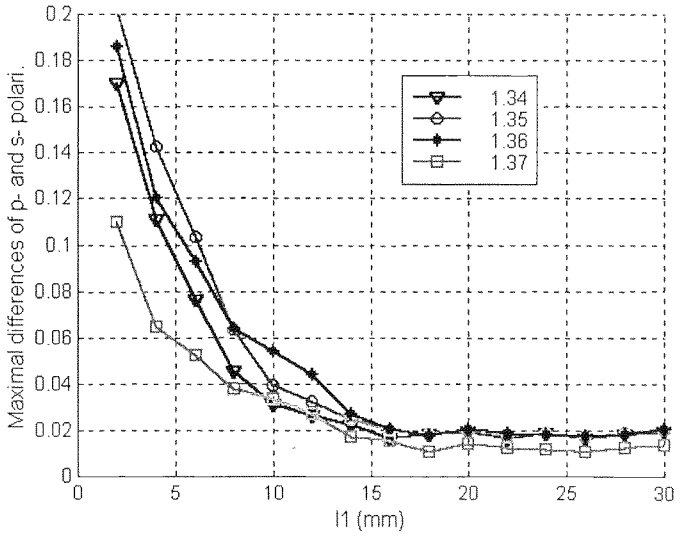

Fig.10 Computed curves of the maximal differences of normalized light power between the p- and the s- polarized illuminations as a function of l_1 (l_s=15mm and l_2=81mm, cf. fig.1. thickness of gold film=55nm, indices of monitored bulk media=1.34,1.35,1.36 and 1.37 respectively)

Therefore, a consistent explanation to the experimental phenomena can be achieved using this model. Nevertheless, the difference of p- and s- polarization illuminations is indeed existent. To neglect the influences of p- and s- polarization of the incident light leads to an uncertainty of about 0.02 to the normalized light power detected at output end of the fiber. Otherwise, while the SPR sensing part moves close to the input end of the fiber, the influences of the polarization become important.

4.3 Quantitative interpretations of the sensing signals

Since surface plasmon resonance (SPR) is particularly sensitive to the small changes either in the geometry or the dielectric properties of the metal-dielectric interface, this kind of SPR fiber-optic sensor is expected to many applications, for example, to monitor the variations of the refractive index of bulk medium or to evaluate the absorption or desorption of surface molecular layer, etc..

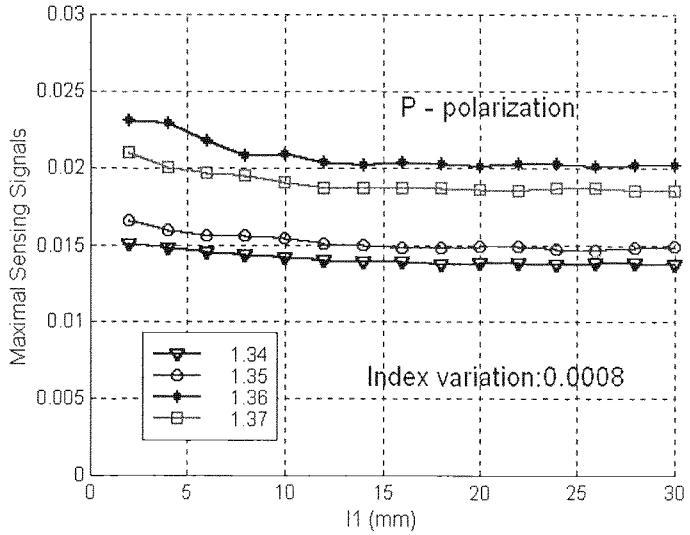

Fig.11 Computed curves of the maximal sensing signals as a function of l_1 (l_s=15mm and l_2=81mm, thickness of gold film=55nm, index variation of 8×10^{-4} in bulk media with indices of 1.34, 1.35, 1.36 and 1.37 respectively)

The sensing signals of the sensor are defined as the variations of the normalized light power transmitted out of the fiber caused by the variations of the monitored parameters. The maximal sensing signal is the maximum of sensing signals occurring between the incident

angles of 5° and 20° where the sensing signals are most notable. Assuming that the sensor is used to monitor the bulk environments of the refractive indices of 1.34, 1.35, 1.36 and 1.37 respectively and the incident light is set to be p-polarization, a change of the index of 8×10^{-4} in each detected bulk medium occurs, the maximal sensing signals as a function of l_1 can be predicted by means of this model and shown in figure 11. Similarly, if a 1nm thick molecular layer with index of 1.46 adsorbs on the surface of gold film in the same bulk environments, the maximal sensing signals as a function of l_1 are plotted in figure 12. The l_s and l_2 are assumed to remain unchanged in these two examples. It can be seen from Fig.11 and Fig.12 that the maximal sensing signal in this two cases is about 0.02 as l_1 >16mm.

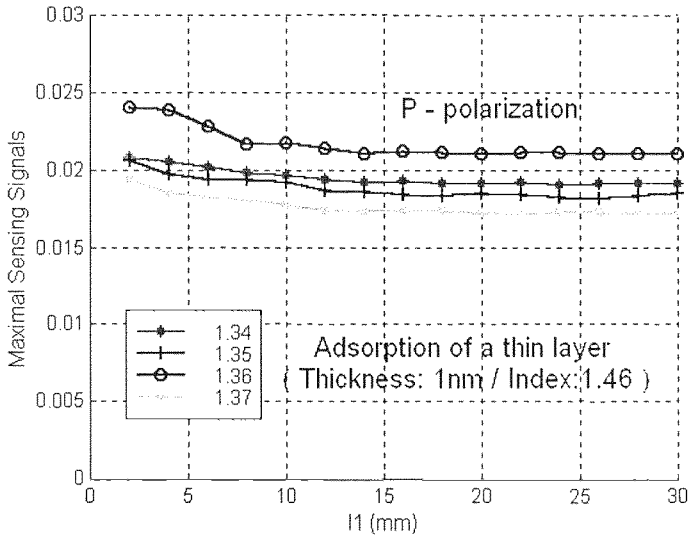

Fig.12 Computed curves of the maximal sensing signals as a function of l_1 (l_s=15mm and l_2=81mm, thickness of gold film=55nm, an adsorbed layer of 1nm thickness with index of 1.46 on the gold surface in bulk media with indices of 1.34, 1.35, 1.36 and 1.37 respectively)

Comparing with the previous result that the possible error is as great as 0.02 while l_1 > 16mm if the influences of polarization of the incident light are ignored, it can be recognized that this error is approximately equivalent to a possible uncertainty in refractive index of 8×10^{-4} for the detected bulk media or in the thickness of 1nm (with index of 1.46) for the adsorbed dielectric layer. Therefore, when a weak sensing signal needs to be quantitatively interpreted, the influences of the polarization for the incident light should not be neglected

and this 3D model must be used. An application to evaluate a 1.77nm thick (index of 1.463) self-assembled monolayer (SAM) will be discussed in another paper.

5. Conclusions

In order to consistently explain the experimental results, a 3D model for accurate description of the properties of an intrinsic multimode fiber optic sensor has been developed. The polarization of the light source has not much influence while the SPR transducer is far from the input end of the fiber. Nevertheless, the accurate model is proposed to use if the small sensing signals need to be quantitatively interpreted. Moreover, while the SPR sensing part is located near to the input end of the fiber that is applicable to a portable fiber-optic sensor, the effects of the polarization are evident. More knowledge about the fashion of light propagation and the performances of the multimode fiber-optic sensors has been acquired. Theoretical studies are ready to quantitatively interpret the sensing signals coming from such as the adsorption of a very thin dielectric layer on metal surface or the slight variation of the refractive index in the monitored bulk medium.

References

1. M.Archenault, H.Gagnaire, J.P.Goure and N.Jaffrezic-Renault, A simple intrinsic optical fibre refractometer, Sensors and Actuators B, 5(1991) 173-179

2. A.Abdelghani, J.M.Chovelon, N.Jaffrezic-Renault, C.Ronot-Trioli, C.Veillas and H.Gagnaire, Surface plasmon resonance fibre-optic sensor for gas detection, Sensors and Actuators B, 38-39(1997) 407-410

3. C.Ronot-Trioli, A.Trouillet, C.Veillas, A.El-Shaikh and H.Gagnaire, Fibre optic chemical sensor based on surface plasmon monochromatic excitation, Analytica Chimica Acta, 319(1996) 121-127

4. A.Trouillet, C.Ronot-Trioli, C.Veillas and H.Gagnaire, Chemical sensing by surface plasmon resonance in a multimode optical fibre, Pure Appl. Opt. 5(1996) 227-237

5. R.C.Jorgenson and S.S.Yee, A fiber-optic chemical sensor based on surface plasmon resonance, Sensors and Actuators B, 12(1993) 213-220

6. Ady Arie, Reuven Karoubi, Yigal S.Gur and Moshe Tur, Measurement and analysis of light transmission through a modified cladding optical fiber with applications to sensors, Appl. Opt. 25(1986) 1754-1758

7. A.Cozannet and M.Treheux, Skew rays in optical fibers, Appl. Opt. 14(1975) 1345-1350

8. K.L.Kliewer and R.Fuchs, Collective electronic motion in a metallic slab, Phys. Rev., 153(1967) 498-512

9. A. Cozannet, H.Maitre, J.Fleuret and M.Rousseau, Optique et télécommunications, Eyrolles(1981,Paris), p.209

10. M.Bron and E.Wolf, Principles of Optics, Third(revised)edition, Pergamon Press, p.38

11. K.Kurosawa, R.M.Pierce, S.Ushioda and J.C.Hemminger, Raman scattering and attenuated-total-reflection studies of surface-plasmon polaritons, Phys. Rev. B, 33(1986) 789-798

Biographies

Wen Bin LIN received B.S.and M.S. degrees in electrical engineering from Zhejiang University in Hangzhou, P.R.China in 1985 and 1988 respectively. Then he jointed the department of electronic science of Nankai University in Tianjin as a researcher and teacher in the fields of electron & ion optics and computer numerical simulation. He was appointed associate professor of electronics in 1995. Since March 1997, he has been a Ph.D. candidate in the laboratory of Ingenierie et Fonctionalisation des Surface in Ecole Centrale de Lyon, France, owing to the scholarship granted by the National Education Committee of China. He works currently in the development of the fiber-optic sensors for the physical, chemical and biological applications.

Nicole Jaffrezic-Renault received engineering degree from the Ecole Nationale Supérieure de Chimie, Paris, in 1971 and the Doctorat d'Etat és Sciences Physiques from the University of Paris in 1976. She jointed the laboratory of Ingenierie et Fonctionalisation des Surface in Ecole Centrale de Lyon, France in 1984 and now she is deputy director of this laboratory. Director of research at the Centre national de la Recherche Scientifique and the president of the chemical micro sensor club (CMC2), her research activities include the preparation and

physicochemical characterization of membranes for chemical sensors (ISFETs, optical fiber sensors, etc.).

Alain Gagnaire received Doctor degree in Physics (specialty in spectroscopy) in 1968 and the Doctorat d'Etat és Sciences Physiques in 1986 from the University of Lyon, France. He jointed Ecole Centrale de Lyon as a lecturer in 1968. As researcher in the laboratory of Electronique Optoelectronique et Microsystems, his principal interests are ellipsometry, thin films for optical applications and optoelectronics.

Henri Gagnaire received the degree of Doctor third cycle in chemistry in 1975 from the Ecole Nationale Supérieure des Mines de Saint-Etienne and the degree of Doctor in Physics in 1985 from the University of Saint-Etienne. Professor in Saint-Etienne University, his research interest is in optics and more recently in optical fiber sensors.

Résonance de plasmon de surface sur fibre optique pour la détermination de l'épaisseur et des constantes optiques de films métalliques minces

Résumé Article 3

Résonance de plasmon de surface sur fibre optique pour la détermination de l'épaisseur et des constantes optiques de films métalliques minces

La mesure de l'épaisseur et des constantes optiques d'un film métallique très fin, d'environ 40 à 70 nm, n'est pas une chose simple ; les influences de sa surface et celle du substrat sont grandes. C'est encore plus difficile lors que ce film métallique est déposé sur un substrat incurvé. Ce qu'il est possible de faire dans ce cas, c'est de mesurer un film métallique équivalent, déposé sur une surface plane, par ellipsométrie ou par réflectométrie. Les inconvénients sont grands puisque, en plus d'une procédure expérimentale longue, il est très difficile d'avoir deux films identiques par évaporation thermique car les paramètres optiques du film dépendent fortement du procédé d'élaboration.

Une méthode directe pour évaluer l'épaisseur et la constante diélectrique du film métallique sur la surface du cœur d'une fibre a été développée dans cet article. Un seul ensemble de solutions peut être obtenu à partir de la mesure des réponses d'un capteur SPR à fibre optique. La fiabilité de cet ensemble de solutions est vérifiée et les erreurs théoriques des paramètres évalués pour le film d'or mesuré sont d±2%, ε_r±1% et ε_i±15%.

La détermination exacte de l'épaisseur et la constante optique du film métallique fournit une possibilité d'optimiser le capteur SPR à fibre optique pour différentes applications et de caractériser les films diélectriques recouvrant la surface du métal tels que des films chimiques ou biologiques pour des applications de détection.

Preface to article 3

Fiber-Optic Surface Plasmon Resonance for Determination of Thickness and Optical Constants of Thin Metal Films

To measure the thickness and the optical constant of a very thin metal film as thick as about 40-70nm is not a easy thing in considering the influences of its surfaces and the substrate. It is much more difficult as this metal film is on a curved substrate. As far as we know, all we can do in this case, is to measure the compared metal film deposited on a plane static substrate by using ellipsometry or reflectometry. The disadvantage is evident since, in addition to a long experimental procedure, it is too difficult to have an identical one by thermal evaporation, while the optical parameters of the thin evaporated film strongly depend on its elaboration process.

A direct method for evaluating the thickness and the dielectric constant of a metal film on the surface of the fiber core has been realized in this paper. An unique set of solutions can be drown out by the measurements of its own fiber-optic surface plasmon resonance (SPR) responses alone. The reliability of the set of solutions is verified and the theoretical errors of the evaluated parameters for the experimental gold film are as within d ±2%, ε_r ±1% and ε_i ±15%.

The exactly determination of the thickness and the optical constant of the metal film provides a possibility to optimize the fiber-optic SPR sensor for different purposes and to characterize the dielectric films coated on metal surface such as the chemical and biological functional films for sensing applications.

Fiber-Optic Surface Plasmon Resonance for Determination of Thickness and Optical Constants of Thin Metal Films

Wen Bin LIN[a,b], *Jean Marc CHOVELON*[a,c], *Nicole JAFFREZIC-RENAULT*[a,*]

[a] IFOS, Ecole Centrale de Lyon, 36 Avenue Guy de Collongue, BP163, 69131 Ecully Cedex, France

[b] Electronic Science Department, Nankai University, Tianjin, 30071, China

[c] LACE, University of Claude Bernard Lyon 1, 69622 Villeurbanne, France

[*] ***Corresponding author:*** *Tel: +33 4 72186243; Fax: +33 4 78331577; Email: Nicole.Jaffrezic@ec-lyon.fr*

Abstract: We demonstrate in this paper that the thickness and the dielectric constants of thin gold films deposited on the surface of a fiber core can be quantitatively determined as a single set of solutions by simply measuring the fiber-optic surface plasmon resonance responses. This method is capable of directly characterizing metal film with a curved surface: this is very hard to perform using the conventional optical techniques of reflectometry and ellipsometry. The theoretical errors for the experimental fiber are estimated to be within d ±2%, ε_r ±1% and ε_i ±15%.

Keywords: *Thickness; Dielectric constant; Thin metal film; Surface plasmon resonance; Fiber-optic sensor*

1. Introduction

The study of the optical properties of metals has been an important subject in physics for many decades. The differences in the results reported by different authors have revealed the complexity of this investigation [1-3]. On the other hand, the optical constants available in the literature, which were usually measured from the bulk materials, often differ from the optical properties of thin evaporated films which strongly depend on their formation processes [4-6].

Conventional optical techniques such as reflectometry, ellipsometry and surface plasmon resonance (SPR) can be employed to characterize the metal film. Distinguished from the other optical methods by its simplicity and rather high sensitivity, the SPR technique is particularly suitable to very thin metal film [4-12]. Successful applications to determine the thickness and

dielectric constant of a thin metal layer have been reported in the prism-based Kretschmann configuration [13-15].

In recent years, optical fiber sensors based on surface plasmon resonance, where part of the cladding of the multimode fiber is replaced by multilayered thin films including a metal layer deposited on the core of the fiber, have attracted considerable interest [16-18] owing to their small size, low cost, flexibility and possible use for remote sensing, instead of the bulk prism-based optical systems traditionally employed [4-15]. The commercial success of BIACORE (Sweden) can prove its potential. The thin metal layer acting as the supporter of the SPR has a very important role in the performance of this kind of fiber-optic sensor. Unfortunately, the conventional optical means of ellipsometry and reflectometry can hardly be adapted to measure the thickness and the dielectric constant of the metal film on the surface of the fiber core due to the curvature of its surface. An indirect method, namely evaluating the metal layer deposited on a plane static substrate, usually has to be used. However, in addition to a long experimental procedure, it can seldom provide the same values as those of the metal film on fiber, which is formed by thermal evaporation during the rotation of the fiber.

The thickness and the dielectric constant of a metal film on the surface of the fiber core have been evaluated in this paper by measuring its own fiber-optic SPR responses alone. The reliability of the set of solutions is verified and the theoretical errors of the evaluated parameters for the experimental gold film are estimated. The significance of the evaluated values and the potential applications of this work are discussed.

2. Experiments

2.1 Experimental set-up

The experimental apparatus should satisfy two basic conditions: (1) The light source must be monochromatic because the optical constant ε of the metal is a function of light wavelength; (2) The experimental set-up should be able to measure the light power curve versus the incident angle as the prism-based optical systems work. Hence, some fiber-optic arrangements such as that of R.C.Jorgenson and S.S.Yee [16] and the commercially available BIACORE (Sweden) are inherently incapable of being employed for this purpose.

Our experimental set-up is schematized in figure 1. A collimated laser diode was installed on a rotation stage, which was driven by a stepper motor with one step corresponding to a rotation of 0.028 degree. The parallel monochromatic light beam of 670nm wavelength emitted from the laser diode was injected into the fiber at s-polarization with respect to the input end face of the fiber and the light power transmitted through the fiber was completely

collected with a photodiode. The measurements and data-acquisition were automated by using a computer.

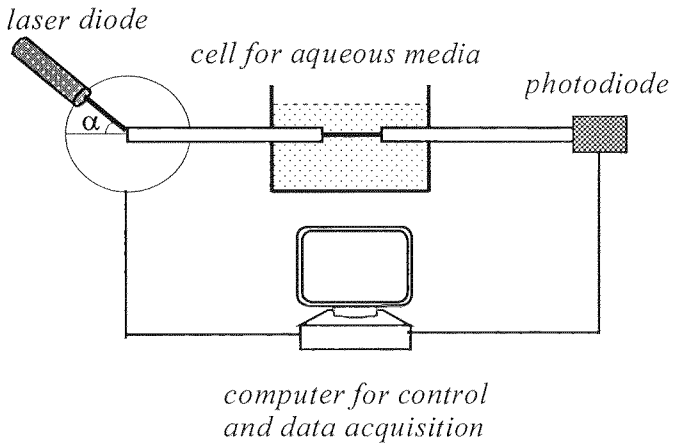

Fig.1. Schematic diagram of the experimental set-up

2.2 Deposition of the gold film on the fiber

The optical fiber tested was a multimode step-index silica/silicone optical fiber (Quartz et Silice PCS 600) with a core diameter of 600μm. A 21cm length of fiber was prepared and its two end faces were carefully polished to minimize the scattering of light. A 15mm section of cladding was removed from the middle of the fiber with a sharp knife and then etched by sulfochromic treatment. Then a section of gold wire [ENGELHARD-CLAL (Paris, France) 99.99% purity] was cut. Both fiber and gold wire were sunk into the acetone solution under ultrasonic conditions for about 15 minutes. After being rinsed in distilled water and dried under nitrogen flow, they were mounted into the vacuum chamber of the evaporation equipment (cf. figure 2). Deposition began after the vacuum reached $2x10^{-6}$ Torr and was kept up during evaporation by using liquid nitrogen. The gold film was coated via thermal evaporation at a rate of 2-6Å/s (reading of the quartz-crystal detector), while the fiber was rotated at a velocity of 50 turns/minute in order to obtain a symmetrical gold film around the fiber core. The expected thickness on the fiber (d) can be controlled by the thickness monitored by the quartz-crystal detector (d_q) with the relation $d = d_q/\pi$.

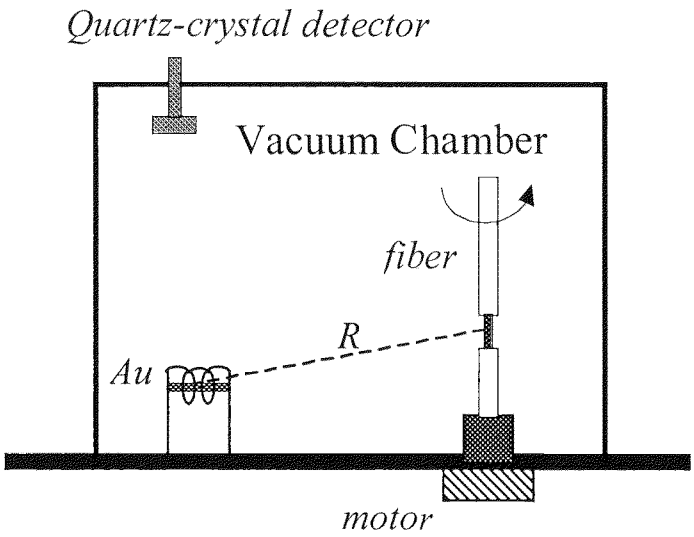

Fig.2. Schematic representation of the vacuum chamber for evaporation

3. Determination of the optical parameters of the metal film

3.1 Brief description of the computational model

An accurate 3D model for ideal multimode fiber-optic sensors was developed in a former paper [18]. The uncladded section of the fiber can be treated as a one dimensional planar multilayered configuration, and the reflectivity to both p- and s- polarized electric field components can be calculated by the matrix method [19]. The input end face of the fiber illuminated by the parallel incidence of the polarized light was divided into numerous small parts. Each skew ray carrying light power from one of these small parts propagates into the fiber and reflects many times with its own trajectory. The variation of the electric field direction and modification of the light energy are taken into account at each reflection. The light power transmitted out of the fiber is yielded by accumulating the output light energy of all skew rays. Interested readers should refer to Ref. 18 for details.

3.2 Characterization of the fiber

The refractive indices of core and cladding are known to be 1.457 and 1.407 respectively. The inherent energy loss of the practical optical fiber is dealt with by introducing the

imaginary part of the refractive index of the cladding. In order to minimize errors coming from the fiber itself, the fiber prior to deposition of the metal film was measured in air atmosphere at room temperature. The imaginary part of the refractive index of the cladding was determined as 2.718×10^{-5} by the least-square fitting of the experimental data (see figure 3). This value was affected by the flaws in the fiber, the slight roughness of its two end faces and the ambient temperature, etc..

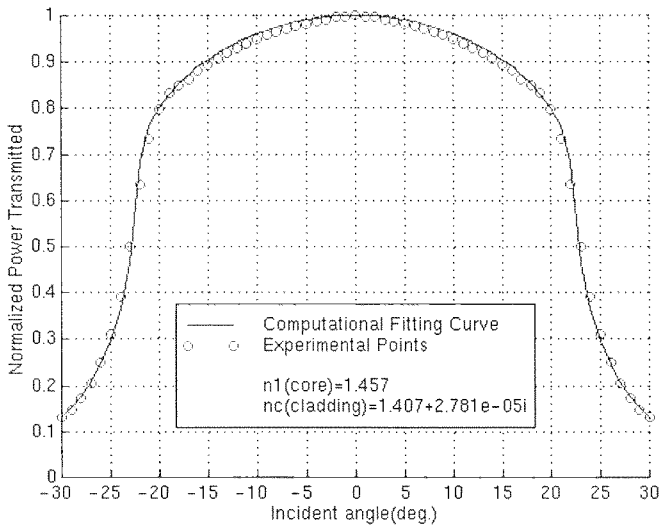

Fig.3. The least-square fitting for determining the imaginary part of the refractive index of the cladding

3.3 SPR measurements in aqueous media

After 2 days of stabilization for the metal film exposed to air at room temperature, the fiber was mounted on the experimental set-up (cf. figure 1). The measurements were performed in transparent aqueous media with well-defined indices of 1.34, 1.35, 1.36 and 1.37 respectively, obtained by mixing ethylene glycol (n=1.431 /20°C) with distilled water (n=1.333 /20°C) and monitored independently by an Abbe refractometer. The SPR manifests itself as a dip in the curve of the incident angular dependence of the transmitted light power. All experimental data is treated by mean square regression in order to reduce the experimental errors, and then normalized.

3.4 Characterization of the gold film

The metal film is characterized by three parameters: the thickness (d), the real part (ε_r) and imaginary part (ε_i) of the dielectric constant ($\varepsilon = \varepsilon_r + i\,\varepsilon_i$). The objective function can be set as the maximal absolute deviation between the computational and the experimental values at incident angles between 1° and 20° for all four curves corresponding to four indices of the measured aqueous media of 1.34, 1.35, 1.36 and 1.37 respectively. In the iteration process, the d, ε_r and ε_i are varied to make the objective function minimal.

Since any variations of d, ε_r and ε_i will lead to changes in the relative positions of the four computational curves, these parameters are mainly determined by the relative shapes of the four experimental curves. Therefore, the solutions of d, ε_r and ε_i are not sensitive to random experimental errors.

The results are shown in figure 4. The maximal deviation reaches a minimum of 0.015. The thickness of the gold film is derived as 619Å and the dielectric constant at 670nm wavelength is –15.89+i 1.31.

The thickness indicated by the quartz-crystal detector is d_q=1890Å, meaning that the thickness of the metal film on the fiber is d=602Å (refer to **2.2**). This value agrees well with the derived thickness of 619Å, with a relative error of 2.8%.

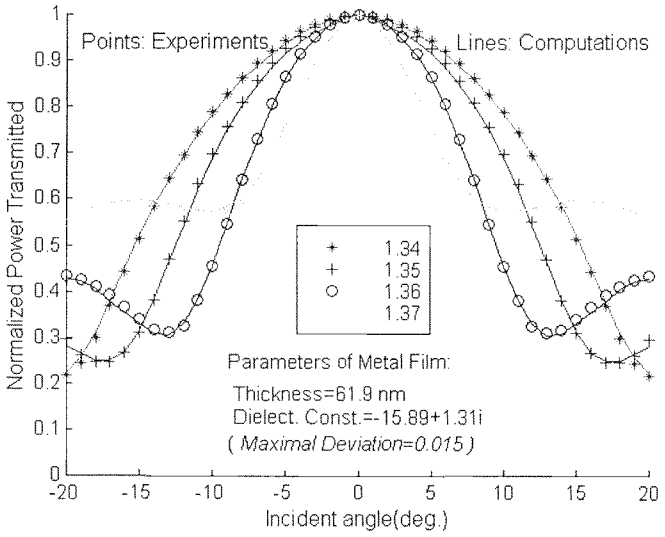

Fig.4. Numerical fitting of experimental curves measured in aqueous media with refractive indices of 1.34, 1.35, 1.36 and 1.37 respectively for determining the metal film parameters (light wavelength of 670nm, maximal deviation of 0.015 between measurement and computation)

3.5 Reliability and uncertainty

The contour maps of the objective function calculated in the vicinity of the computed parameters (d=619Å and $\varepsilon = -15.89+i\ 1.31$) are depicted in figures 5(1), 5(2) and 5(3). They prove that the iteration process is convergent in their solution vicinities and the results are unique whatever the initial values and the iterative order of parameters d, ε_r and ε_i .

The uncertainties for d, ε_r and ε_i can be estimated from the figures above as well. In case of the maximal deviation of 0.015, the maximal uncertainties are about 12Å for the thickness, 0.18 for the real part and 0.19 for the imaginary part of the optical constant. Hence, the relative errors are within 2% for the thickness, 1% and 15% for the real part and the imaginary part of the optical constant respectively.

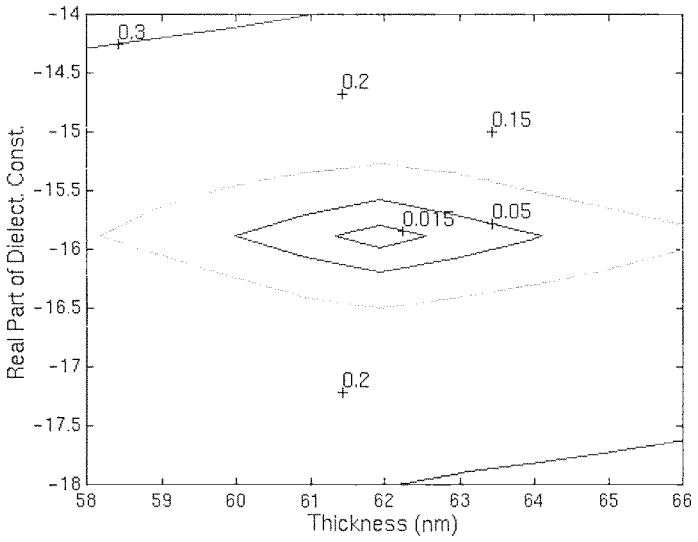

Fig.5(1). The contour map of the objective function vs. d and ε_r at ε_i =1.31

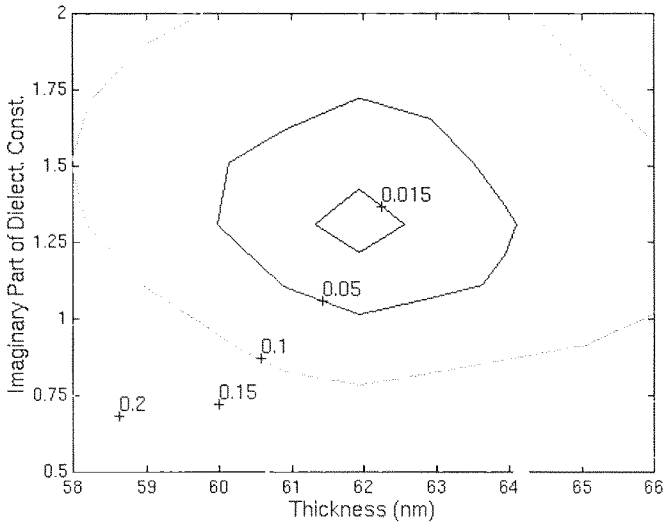

Fig.5(2). The contour map of the objective function vs. d and ε_i at ε_r = -15.89

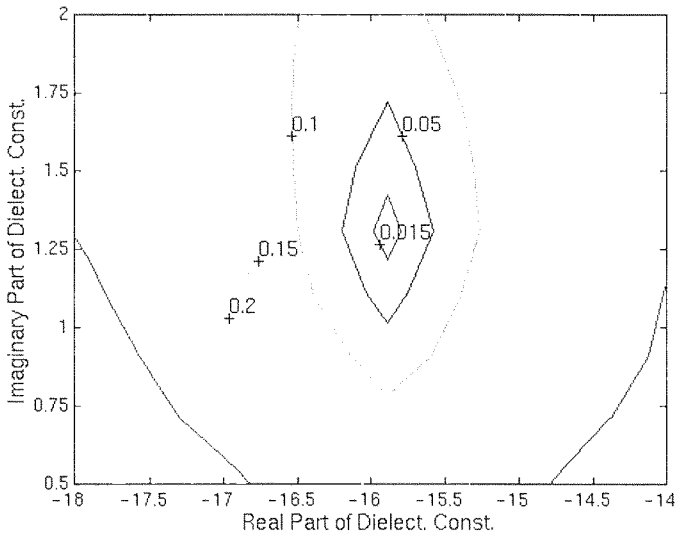

Fig.5(3). The contour map of the objective function vs. ε_r and ε_i at d =619Å

Other computations demonstrated that the number of aqueous media to measure and the choice of their index values would affect the accuracy of the computational results. Only one

SPR curve can not offer adequate information to simultaneously determine three parameters of the metal film.

4. Comparison with experiments at another wavelength

The purpose of this comparison is to examine the reliability of our work. Since the thickness of the metal film is independent of light wavelength, the derived thickness at different light wavelengths must be identical.

The same fiber was measured once again using another laser diode with a wavelength of 658nm. The optical parameters of the metal film are obtained, by the same procedure as before, as a set of solutions of d=614Å and $\varepsilon = -14.65+i\ 1.35$. The experimental and computational curves are plotted in Figure 6. This thickness of 614Å (±11Å) is almost the same as d=619Å (±12Å) obtained at a wavelength of 670nm. Our work can therefore be considered reliable.

Moreover, the derived dielectric constants are examined. Although the optical parameters of the evaporated thin metal film are known to be usually different to the data of the literature due to the different film formation process, the wavelength dependent tendency of the dielectric constants is in close agreement with that of ref.3 and ref.20 (see figure 7). In both references a metal film as thick as several dozen nanometers evaporated on a planar surface is investigated. The method of "transmission-interference-filter" proposed in ref.3 can be used to independently determine the absorption coefficient (k) and the refraction index (n) which are associated with the complex dielectric constant ε by $\varepsilon=(n+i\ k)^2$. Ref.20 is of more interest in comparison with our work since it utilizes the same SPR probe but in the traditional prism-based Kretschmann geometry. Actually, our results are closer to those of ref.20.

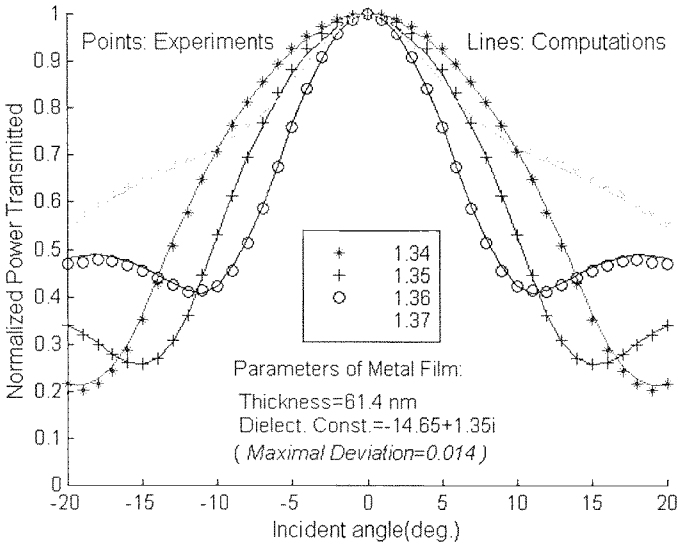

Fig.6. Numerical fitting of experimental curves measured in aqueous media with the refractive indices of 1.34, 1.35, 1.36 and 1.37 respectively for determining the metal film parameters (light wavelength of 658nm, maximal deviation of 0.014 between measurement and computation)

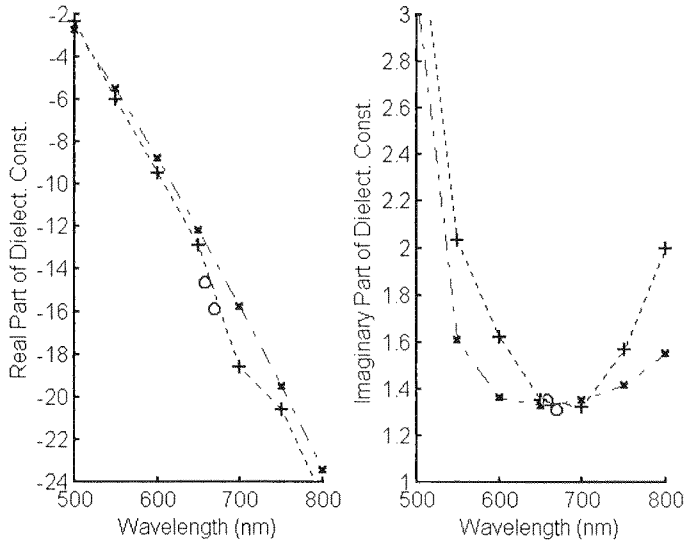

Fig.7. Comparison of our results of dielectric constants at wavelengths of 658nm and 670nm (marked "o") with those of L.G.Schulz [3] (marked "x" and linked with dashed line) and R.A.Innes and J.R.Sambles [20] (marked "+" and linked with dotted line)

5. Discussion

Considering that the fiber-optic SPR responses at different incident angles embodying information about the metal film are the signals carried by a wide variety of skew light rays which propagate through the fiber along different trajectories and reflect several times with various incident angles on the whole core-metal film interface, it should be recognized that it is the optical parameters spatially averaged over entire metal film that are determined. However, in traditional prism-based optical system, since the light beam hits only a small area of the metal surface [13-15], only the values averaged over this small illuminated area are given.

A homogeneous and isotropic metal film with ideal smooth and parallel interfaces is assumed in the theoretical computations. Unfortunately, the evaporation rate, which associates the inclusion degree of oxygen and water vapor in the deposited metal film [4,5], can hardly be kept constant, leading to non-homogeneity of the metal layer. A somewhat oblique incidence of the gold atoms to the curved surface of the fiber core during the formation of the metal film results in a porous surface region with a preferred structural direction defined as the surface anisotropy[6]. Moreover, an evaporated metal film has natural roughness [21]. Therefore, it must be understood that the parameters of the metal film obtained in this paper are the effective and average thickness and dielectric constant of the whole metal film on the fiber.

Nevertheless, knowledge of these quantities is very useful in view of practical applications. It helps us to understand, then control to some degree, the optical performance of evaporated metal films, and makes it possible to optimize the fiber-optic surface plasmon resonance sensor for different purposes, to characterize the dielectric films coated on a metal surface such as chemical and biological functional films, and to quantify the monitored parameters in a sensing application.

Acknowledgements

The authors thank Mr. Denis DESCHATRE for installing the system of metallic deposition on optical fiber in the vacuum thermal evaporation apparatus in the IFOS laboratory, Ecole Centrale de Lyon, France. They also thank Mrs. Colette VEILLAS for her help in performing some of the SPR measurements at the TSI laboratory, Jean Monnet University in Saint-Etienne, France.

References

1.M.A.Ordal, L.L.Long, R.J.Bell, S.E.Bell, R.R.Bell, R.W.Alexander, Jr., and C.A.Ward, "Optical properties of the metals Al, Co, Cu, Au, Fe, Pb, Ni, Pd, Pt, Ag, Ti, and W in the infrared and far infrared," Appl. Opt. 22, 1099-1119(1983)

2. P.B.Johnson and R.W.Christy, "Optical constants of the noble metals," Phys. Rev. B 6, 4370-4379(1972)

3. L.G.Schulz, "The optical constants of Silver, Gold, Copper and Aluminum. I. The absorption Coefficient k," J. Opt. Soc. Am., 44(1954), 357-362; and L.G.Schulz and F.R.Tangherlini, "The optical constants of Silver, Gold, Copper and Aluminum. II. The index of refraction," J. Opt. Soc. Am. 44, 362-368(1954)

4. W.H.Weber and S.L.MaCarthy, "Anomalies in the surface plasmon resonance excitation at both surfaces of evaporated metal films," Appl. Phys. Lett. 25, 396-398(1974)

5. E.Fontana, R.H.Pantell, and M.Moslehi, "Characterization of dielectric-coated, metal mirrors using surface plasmon spectroscopy," Appl. Opt. 27, 3334-3340(1988)

6. W.H.Weber and S.L.McCarthy, "Surface-plasmon resonance as a sensitive optical probe of metal-film properties," Phys. Rev. B 12, 5643-5650(1975)

7. T.Lopez-Rios and G.Vuye, "Use of surface plasmon excitation for determination of the thickness and optical constants of very thin surface layers," Surf. Sci. 81, 529-538(1979)

8. E. Fontana, R.H.Pantell, "Characterization of multilayer rough surfaces by use of surface plasmon spectroscopy," Phys. Rev. B 37, 3164-3182(1988)

9. H.Kitajima, K.Hieda and Y.Suematsu, "Optimum conditions in the attenuated total reflection technique," Appl. Opt. 20, 1005-1010(1981)

10. H.Gugger, M.Jurich and J.D.Swalen, "Observation of an index-of-refraction-induced change in the Drude parameters of Ag films," Phys. Rev. B 30, 4189-4195(1984)

11. C.E.Reed, J.Giergiel and S.Ushioda, "Effects of annealing on the attenuated-total-reflection spectra of cold-evaporated silver films," Phys. Rev. B 31, 1873-1880(1985)

12. X.Sun, S.Shiokawa and Y.Matsui, "Interactions of surface plasmons with surface acoustic waves and the study of the properties of Ag films," J. Appl. Phys. 69(1), 362-366(1991)

13. Helene E.de Bruijin, Rob P.H.Kooyman and Jan Greve, "Determination of dielectric permittivity and thickness of a metal layer from a surface plasmon resonance experiment," Appl. Opt. 29, 1974-1978(1990)

14. F.Yang, Z.Cao and J.Fang, "Use of exchanging media in ATR configurations for determination of thickness and optical constants of thin metallic films," Appl. Opt. 27, 11-12(1988)

15. W.P.Chen and J.M.Chen, "Use of surface plasmon waves for determination of the thickness and optical constants of thin metallic films," J. Opt. Soc. Am. 71, 189-191(1981)

16. R.C.Jorgenson and S.S. Yee, "A fiber-optic chemical sensor based on surface plasmon resonance," Sensors and Actuators B 12, 213-220(1993)

17. C.Ronot-Trioli, A.Trouillet, C.Veillas A.El-Shaikh and H.Gagnaire, "Fibre optic chemical sensor based on surface plasmon monochromatic excitation," Analytica Chimica Acta 319, 121-127(1996)

18. W.B.Lin, N.Jaffrezic-Renault, A.Gagnaire, H.Gagnaire, "The Effects of Polarization of the Incident Light -- Modeling and Analysis of a SPR Multimode Optical Fiber Sensor," Sens. Actuators A, In press

19. K.Kurosawa, R.M.Pierce, S.Ushioda and J.C.Hemminger, "Raman scattering and attenuated-total-reflection studies of surface-plasmon polaritons," Phys. Rev. B 33, 789-798(1986)

20. R.A.Innes and J.R.Sambles, "Optical characterisation of gold using surface plasmon-polaritons," J. Phys. F: Metal. Phys. 17, 277-287(1987)

21. H.Raether, "The dispersion relation of surface plasmons on rough surfaces; A comment on roughness data," Surf. Sci. 125, 624-634(1983)

Observation in situ et caractérisation de monocouches auto-assemblées par plasmon de surface sur fibre optique

Résumé article 4

Observation in situ et caractérisation de monocouches auto-assemblées par plasmon de surface sur fibre optique

Le but de cet article est d'introduire une nouvelle sonde de la surface totale et de présenter son application en chimie.

Il est bien connu qu'un certain nombre de moyens optiques tels que la reflectométrie, l'ellipsométrie et la résonance de plasmon de surface (SPR) peuvent être employés pour étudier des films diélectriques adsorbés. Cependant, les techniques optiques conventionnelles actuellement existantes donnent habituellement accès à des paramètres optiques seulement sur une partie de la surface diélectrique à l'endroit d'impact du faisceau lumineux. Nous proposons dans cet article une sonde à fibre optique basée sur l'excitation SPR par les rayons monochromatique non méridiens, ce qui permet de sonder en temps réel les propriétés effectives intégrées sur l'ensemble de la surface diélectrique. L'application de la technique SPR à fibre optique pour étudier les monocouches auto-assemblées (SAMs) et l'observation directe et la description du procédé d'inclinaison par rapport à la surface au cours de l'auto-assemblage de l'alkylthiol, à notre connaissance, n'ont jamais été rapportés dans la littérature auparavant. Les paramètres statiques, déduits seulement des réponses de la sonde SPR, présentent des valeurs spatialement moyennées sur toute la couche diélectrique. Les résultats expérimentaux (épaisseur, indice de réfraction et angle d'inclinaison des molécules de la couche) sont en accord avec les résultats de la littérature.

La bonne sensibilité obtenue montre que notre approche fibre optique simple et bon marché, très facile d'utilisation, est mieux adaptée que les moyens optiques conventionnels, tels que l'ellipsométrie et le système SPR sur prisme, pour suivre les variations sur tout le film diélectrique sondé. Le fait que les rayons lumineux se propageant le long de la fibre vont se réfléchir sur toute la partie sensible du capteur à fibre optique explique ce phénomène.

Les applications potentielles de cet outil prometteur, non seulement en chimie mais aussi en physique (surfaces et films minces) et en biologie, comme présenté dans l'article suivant, peuvent être envisagées.

Preface to article 4

In Situ Observation and Characterization of Self-Assembled Monolayers by Fiber-Optic Surface Plasmon Resonance

The purpose of this paper is to introduce a novel whole surface optical probe and present its application in chemistry.

It is well known that a number of optical means such as reflectometry, ellipsometry and surface plasmon resonance (SPR) can be employed to study the adsorbed dielectric films. Nevertheless, the conventional optical techniques actually existent usually give the optical parameters over only a part of the dielectric surface where the light beam illuminates it. We propose in this paper a fiber-optic probe based on the monochromatic skew ray excitation of SPR, which is capable of investigating in real time the effective properties over entire dielectric layer. The application of the fiber-optic SPR technique to study the self-assembled monolayers (SAMs) and the direct observation and description of the tilting process during the self-assembly of alkylthiol, to our knowledge, have never been reported before in the literature. The static parameters, derived from its own SPR responses alone, present the spatially averaged values over the whole dielectric layer. The experimental results (the thickness, the refractive index and the molecular tilting angle of the alkylthiol SAM) agree very well to the literature.

The rather high sensitivity proves that our fiber-optic approach simple and inexpensive, very easy to use, is more adapted than the conventional optical means, such as ellipsometry and the prism-based SPR system, to monitor the variations over entire investigated dielectric film. The fact that the light rays propagating through the fiber will hit whole sensitive part of the fiber-optic sensor can explain this phenomenon.

The potential applications not only in chemistry but also in physics such as surface and thin films and in biology as it can be seen in the 5th article can be anticipated by using this promising tool.

In Situ Observation and Characterization of Self-Assembled Monolayers by Fiber-Optic Surface Plasmon Resonance

Wen Bin LIN[a,b], Jean Marc CHOVELON[a,c,*], Monique LACROIX[a], Nicole JAFFREZIC-RENAULT[a]

[a] IFOS, Ecole Centrale de Lyon, 36 Avenue Guy de Collongue, BP163, 69131 Ecully Cedex, France

[b] Electronic Science Department, Nankai University, Tianjin, 30071, China

[c] LACE, Claude Bernard-Lyon 1 University, 69622 Villeurbanne, France

[*] ***Corresponding author:*** *Tel: +33 4 72432638; Fax: +33 4 78331577; Email: chovelon@univ-lyon1.fr*

Abstract: Self-assembled monolayers (SAMs) have been intensively investigated in recent years. Only a few methods are capable of in-situ observation of their formation process. This paper reports on a fiber-optic measurement technique based on surface plasmon resonance that is able to study the real-time adsorption kinetics and evaluate the static optical properties of SAMs. Experiments are carried out to investigate the self-assembly of alkylthiol. The real-time measurement visually demonstrates a 3-step process in its formation, especially the tilting process of the alkylthiol molecules in the third step, which has seldom been observed in-situ. The estimated tilting angle and the experimentally derived optical parameters of the alkylthiol SAM agree well with the literature. This simple SPR fiber-optic approach, very easy to use, is rather sensitive to the variations occurring over entire investigated SAMs.

Keywords: *In situ observation; Characterization; Formation kinetics; Alkylthiol; Self-assembled monolayers; Surface plasmon resonance; Fiber-optic sensor*

1. Introduction

Metal surfaces and their adsorbed films have long been the subject of research. They can be investigated by numerous experimental techniques including surface plasmon resonance (SPR). SPR, which can greatly enhance the electromagnetic field on the metal-dielectric interfaces, is therefore a rather sensitive probe for the modifications occurring near the metal surfaces. Characterization of the adsorbed dielectric layers is usually carried out using the

traditional SPR configuration containing a coupling prism[1-3]. Their formation kinetics especially for biomolecular interaction layers, can be evaluated just as well where a flow cell in close contact with the metal surface and a circulatory system to maintain a closed volume of solution through the cell are necessary[4-6].

A great deal of literature has been published on the behaviors of self-assembled monolayers (SAMs)[7]. SAMs created by spontaneous adsorption are very uniform, oriented and robust. The highly reproducible monolayers with well-defined composition, structure and thickness provide new ways of modifying and controlling the chemical and physical properties of the surface or interface, and many applications can thus be expected in the fields of microelectronics, tribology, biochemistry and nonlinear optics, etc.[8-9]. Nevertheless, relatively little is known about their formation kinetics that offers considerable insight into the growth mechanisms of SAMs[10-12].

In this paper, we introduce a promising SPR-based fiber-optic approach that is capable of in situ and non-destructive observation of the formation and quantitative evaluation of the static structures of the SAMs. It possesses the required high sensitivity owing to the SPR effect, and allows fast and direct measurements since the metal film on the fiber is immersed directly into solutions. The formation process of the alkylthiol SAM is monitored using this fiber-optic arrangement. The tilt phenomenon of the thiol molecule is directly observed and the tilting angle is estimated. Moreover, the optical properties of the alkylthiol SAM are evaluated. The experimental set-up is rather simple, inexpensive and possibly portable, and can be adapted to remote detection.

2. Experiments

2.1 Preparation of the alkylthiol solution and the fiber

The alkylthiol solution was prepared by diluting the 1mM 11-Mercaptoundecanoic acid (synthesized at IBCP-CNRS Lyon, France) in ethanol.

The fiber utilized was multimode step-index silica/silicone optical fiber (Quartz et Silice PCS 600). A length of 21cm fiber was cut and its two ends were carefully polished to minimize the scattering of light. Part of the cladding, 15mm in length at the middle of the fiber, was removed with a sharp knife and then etched with sulfochromic treatment. A gold film (about 40-70nm thick) was deposited on the fiber core via thermal evaporation. After 2 days of stabilization for the metal film exposed to air at room temperature, the fiber was exposed to different diluted ethanol solutions whose indices were monitored independently by Abbe refractometer. The incident angle dependence of the SPR responses was measured to

determine the thickness and the optical constant of the gold film; this has been discussed in another paper[13]. By using these diluted ethanol solutions, contamination of the gold surface can be avoided, so the alkylthiol film can afterwards be studied.

2.2 Experimental set-up

The measurements were performed on the experimental arrangement schematized in figure 1. The fiber was mounted through a small cell containing the experimental solutions. A laser diode installed on a rotator stage, which was precisely driven by a stepper motor, provided a parallel monochromatic light beam with a wavelength of 658nm. The monochromatic light was obliquely injected into the fiber at an external incident angle of α. S-polarization with respect to the input end face of the fiber is adopted since this way is easier to keep a uniform light intensity on the incident face of fiber than that of p-polarization during the measurements of the sensing responses against different external incident angles. The light power transmitted out of the fiber was completely collected by a photodiode. The photovoltage was amplified, giving a reading proportional to the transmitted light power. All controls and the data-acquisition were automated by using the computer.

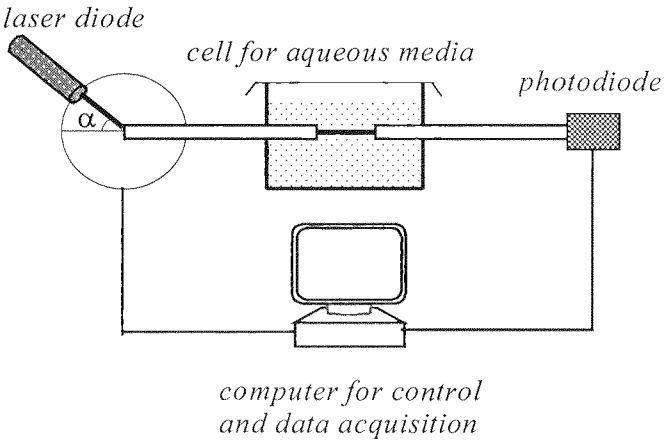

Fig.1. Diagram of the experimental set-up

3. Theory

The SPR phenomenon has been known for many decades[3]. Surface plasmons are the charge density oscillations that propagate along a metal-dielectric interface. These surface

electromagnetic modes excited by transverse magnetic (TM) polarized wave strongly concentrate at the metal surface and decay exponentially into the neighboring phases. This effect makes SPR highly sensitive, so it can detect the very thin SAMs adsorbed on the metal surface.

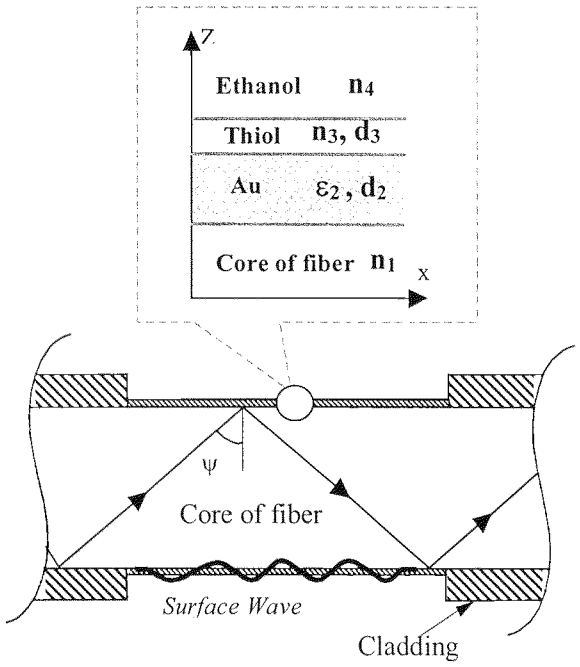

Fig.2. Diagram of the fiber-optic SPR configuration

The sensing part of the fiber-optic SPR configuration applied to study the formation and the characterization of the alkylthiol film in the ethanol solution is illustrated in figure 2. Since the deposited metallic layer (<70nm) and the adsorbed thiol SAM (<2nm) are rather thin compared with their length (15mm) and the diameter of the core of the fiber (600μm), the dielectric layers defined by the parameters of thickness (d) and refractive index (n) or dielectric constant ($\varepsilon=n^2$) can be treated as a one dimension planar geometry. The reflectivity for the p-polarized incident light in this 4-layered configuration can be calculated as[14]:

$$R_p = \left| \frac{(\alpha_4 + \alpha_3)c_3 + (\alpha_4 - \alpha_3)c_4\beta_3}{(\alpha_4 + \alpha_3)c_1 + (\alpha_4 - \alpha_3)c_2\beta_3} \right|^2$$

where

$$c_1=(\alpha_2+\alpha_1)(\alpha_3+\alpha_2)+(\alpha_2-\alpha_1)(\alpha_3-\alpha_2)\,\beta_2$$

$$c_2=(\alpha_2+\alpha_1)(\alpha_3-\alpha_2)+(\alpha_2-\alpha_1)(\alpha_3+\alpha_2)\,\beta_2$$

$$c_3=(\alpha_2-\alpha_1)(\alpha_3+\alpha_2)+(\alpha_2+\alpha_1)(\alpha_3-\alpha_2)\,\beta_2$$

$$c_4=(\alpha_2-\alpha_1)(\alpha_3-\alpha_2)+(\alpha_2+\alpha_1)(\alpha_3+\alpha_2)\,\beta_2$$

and

$$\alpha_j=\varepsilon_j/k_{zj}$$

$$\beta_j=exp(i2k_{zj}\,dj)$$

$$k_{zj}=(2\pi/\lambda)\,(\varepsilon_j-\varepsilon_1\sin^2\psi)^{1/2}$$

λ is the light wavelength; ψ is the internal incident angle of the light ray undergoing in the fiber; j=1,2,3 and 4 indicate respectively the media: "core of the fiber", "gold film", "thiol SAM" and "ethanol solution". The same formulae can be used for calculating the reflectivity of the s-polarized incident light if $\alpha_j=\varepsilon_j/k_{zj}$ is replaced by $\alpha_j=k_{zj}$.

While SPR is excited, part of the energy of the incident light is transferred to the evanescent surface waves, leading to an apparent attenuation of the reflectivity. Therefore, SPR demonstrates itself as a sharp minimum in the curve of the reflectivity versus the internal incident angle. If we assume that the formation process of the alkylthiol layer is described by an increase of its refractive index (n_3) from 1.359 (index of ethanol at 24°C) to 1.463 (index of alkylthiol SAM[15]) with a the thickness (d_3=1.77nm[15]) remaining constant, the evolution of the reflection curves is shown in figure 3 (other parameters used in these calculations are n_1=1.457, ε_2=-13.15+i 1.34, d_2=51nm and n_4=1.359).

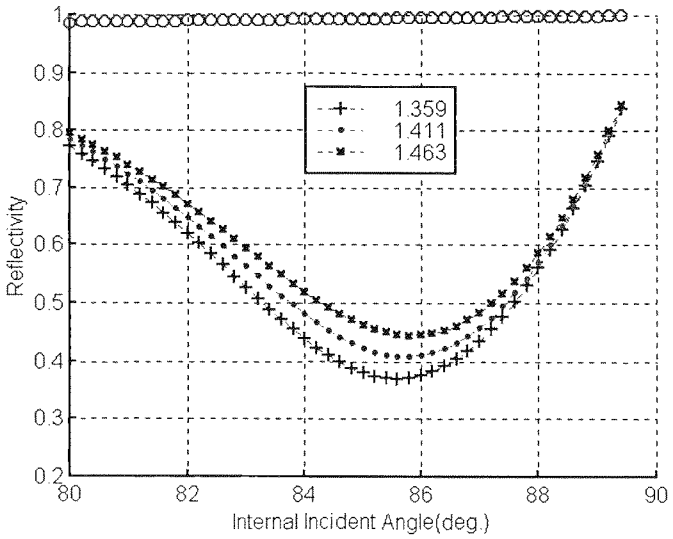

Fig.3. Computational reflectivity versus internal incident angle (ψ) for the 4-medium geometry. The dips in the curves above indicate the existence of the SPR. The formation process of the alkylthiol film is expressed as an increase of its refractive index as n_3=1.359,1.411 and 1.463. The dotted curves refer to the incident light with p-polarization while the straight line of "o"s represents the results of s-polarized light incidence at the same conditions. Other parameters of n_1=1.457, ε_2=-13.15+i 1.34, d_2=51nm, d_3=1.77nm and n_4=1.359 are utilized in these calculations.

However, the measurements of SPR are performed in the experimental set-up presented above. The light rays illuminating the input end of the fiber with a fixed external incident angle α (cf. Fig.1) will propagate into the fiber with a distribution range of the internal incident angle ψ. For example, the skew rays with ψ=83.2°-90° correspond to α=10° according to the relation of $\cos\psi=(\sin\alpha\cos\beta)/n_1$ (where β=0°~90°, referred to equ.(1) in [16]), in which 90% of light energy is dispersed in the range of ψ=83.2°-87.0°. Therefore the input end face of the fiber is divided into many small parts in order to calculate the light power transmitted out of the fiber. Each skew ray carrying the light power of one of these small parts passes into the fiber and reflects many times with its own trajectory. The responses detected at the end of the fiber are obtained by accumulating the output light energy of all skew rays[16]. Hence, the feasibility of observing the formation process of alkylthiol film using this fiber-optic SPR arrangement can be predicted according to the computational

results plotted in figure 4, where the left-hand figure visually indicates that there is a sensitive region in the vicinity of 10° with regard to the external incident angle in which the maximal detectable signal, i.e. the maximal variation of the normalized light power measured at the end of the fiber, can be obtained. The right-hand figure clearly demonstrates that this detectable signal varies in proportion to the variation of the monitored refractive index (the same as to the variation of thickness) of the alkylthiol film. The conclusion is that the alkylthiol formation kinetics can be observed in-situ by fixing the external incident angle at about α=10° and by measuring the variation of the output voltage which is proportional to the transmitted light power.

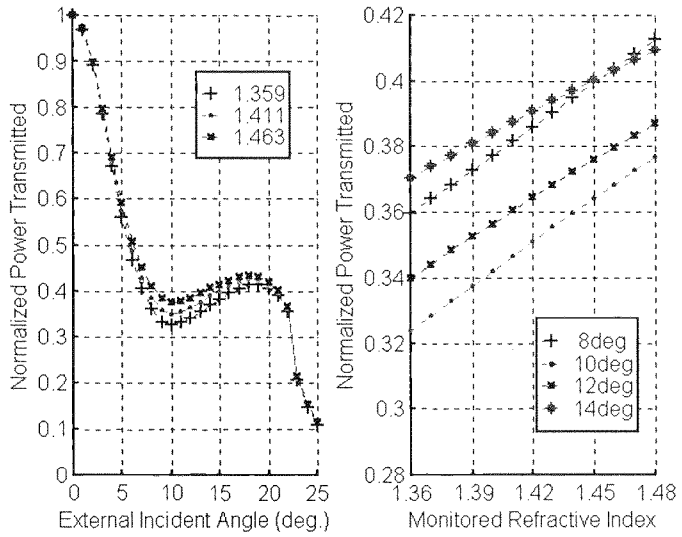

Fig.4. Computational normalized light power transmitted out of the fiber versus external incident angle α with n_3=1.359,1.411 and 1.463 respectively (see left-hand figure) and versus the refractive index of n_3 with α=8, 10, 12 and 14 (degree) respectively (see right-hand figure). Other parameters used in these calculations are n_1=1.457, d_2=51nm, ε_2=-13.15+i 1.34, d_3=1.77nm and n_4=1.359. In addition, index of the cladding is assumed to be $1.407+2.781\times10^{-5}$i[13].

4. Results and discussion

4.1 Formation kinetics

The kinetics of the self-assembly of alkylthiol was recorded with α=10° relative to the axis of the fiber. The environment temperature was maintained at a constant 24°C during the 10-

hour-long experiments. The thiol solution was injected into the small cell when timing began. A magnetic stirring system was introduced in order to keep the alkylthiol solution homogeneous. The reading of the voltage, proportional to the light power transmitted out of the fiber, was automatically acquired every 2 minutes under the control of the computer programs. The variations of the monitored voltage relative to its initial value (noted as ΔV), which completely results from the evolution of the alkylthiol film over the gold surface if the experimental background noise can be neglected, were plotted in figure 5.

The adsorbed layer can be characterized by two optical parameters as the thickness and the refractive index. Unfortunately, the chemical process of the SAM formation is rather complicated[17], both the thickness and the refractive index may vary during its formation.

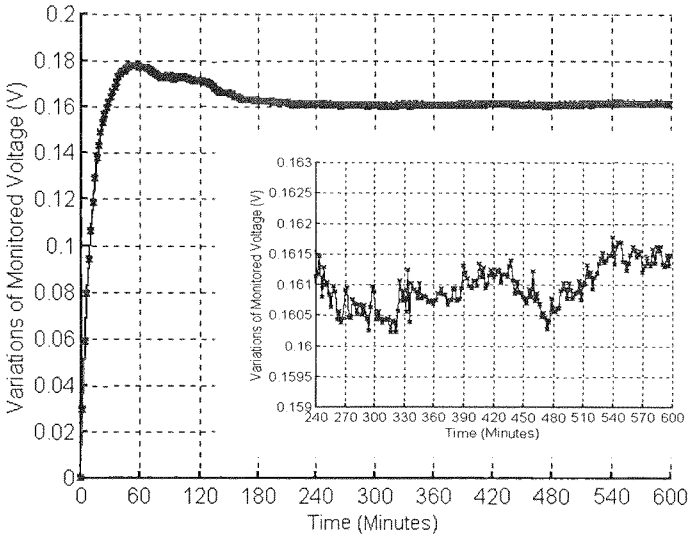

Fig.5. The time dependent variations of the monitored voltage, presenting the formation kinetics of the alkylthiol film with a 3-step process

According to the experimental curve in figure 5, the dynamic formation process of the alkylthiol film can be interpreted as three steps with different time constants. The first step corresponding to the rising part of the experimental curve implies an adsorption process while a great number of thiol molecules move towards and concentrate on the clean surface of the gold film. The surface coverage of the thiol molecules quickly increases and reaches 80-90% of its final value in the first 20 minutes. The adsorption progressively slows down until the

gold surface is saturated after exposure to the thiol solution for about one hour: this is defined as the second step. During this step, the solvent molecules are removed from the gold surface; meanwhile lateral diffusion of the adsorbed thiol molecules on the gold surface takes place. The implanted thiol molecules remain outstretched and perpendicular to the metal surface to facilitate the incorporation of the following thiol molecules. The film is gradually reinforced, implying an increase in the refractive index of the film. The third step, lasting about 3 hours and manifesting itself by a drop in the experimental curve, strongly suggests a thinning of the alkylthiol film, since the alkylthiol molecules have so fully covered the gold surface that the refractive index of the alkylthiol film associated with its molecular density should remain constant in this period. This decrease in thickness is attributed to the tilt of the molecules. Indeed, after the saturation of the film, the molecules will tilt in order to minimize their free volume, thereby minimizing the free surface energy of the system[18]. In fact, the tilting process in the SAM formation has been recognized in literature for a long time but seldom been observed in real time by experiments. After these three steps lasting about 4 hours in total, the curve presents almost a straight line. It means that thermodynamic equilibrium has been reached and a uniform and oriented alkylthiol SAM has been realized.

Experimental background noise as low as 1.5mV can be estimated as the maximal fluctuation of ΔV observed in the period between 4 hours and 10 hours (see Fig. 5). This part of the experimental curve confirms that the alkylthiol SAM is rather stable, and no additional layers are constituted in our case.

As discussed above, the variation of the thickness of the alkylthiol film is proportional to the variation of the detected light power during the tilting process of the thiol molecules. Therefore, the tilting angle with respect to the normal of the gold surface, denoted as θ, can be estimated according to the relation of $\cos\theta = \Delta V_f / \Delta V_m$, where ΔV_m and ΔV_f are the maximum and the final value of ΔV respectively (cf. figure 5). On the basis of our experimental recordings, ΔV_m=0.1776V and ΔV_f=0.1610V (the average value of ΔV between 4 and 10 hours) result in a tilting angle of 25.0°. This value is in very good agreement with the literature[18].

Notice that the signals provided here are associated with the spatially averaged information of the whole adsorbed film on the metal surface since the skew rays propagate with different trajectories and hit the metal surface several times with a dispersed range of the internal incident angles[16], while for the traditional prism-based optical SPR arrangement[1-6] only the part of the metal surface is illuminated and thus is investigated. Therefore, this is a real

advantage of our fiber-optic SPR approach over the bulk prism-based SPR system, for the average effects over whole adsorbed films can be studied.

Although our experiments alone cannot give us an accurate and complete description at the molecular level of the internal process of the SAM conformation, it indeed offers the morphological information on the evolution of SAM, and clearly indicates the function-dependent time intervals during its formation by this very easy and adequately sensitive way.

It is known that many factors such as the ambient temperature, the concentration of thiol molecules in solution and the contamination on the metal surface, etc. can affect the formation of the SAMs and consequently alter the experimental curves. Therefore, some parameters such as the time interval in each step will be modified if the experimental conditions vary.

4.2 Characterization of the alkylthiol SAM

After the completion of the alkylthiol film, the fiber was rinsed with distilled water and dried in nitrogen flow. Then it was exposed to the ethanol solution and the transmitted light power was measured against the incident angles of light. The evaluated thickness of this SAM is derived from the best fit of the computational data to the experimental curve while its refractive index is set as some known values. Figure 6 plots the evaluated thickness of the alkylthiol film as a function of its refractive index.

The refractive index of this alkylthiol SAM has been theoretically estimated as 1.463[15]. The corresponding thickness can be determined from the curve of figure 6 as 17.1Å. Taking the tilting angle of 25.0° obtained above into consideration, the fully extending molecules perpendicular to the gold surface can be found to be as long as about 18.9Å. The relative deviation of this value to the theoretical thickness of the fully stretched molecule known as 17.7Å[15] is only 7%.

In addition, computations demonstrate that a fiber-optic SPR experimental curve is not able to offer adequate information to determine independently both the thickness and the refractive index of the adsorbed monolayer. This is similar to the case of single-wavelength ellipsometric measurements[9].

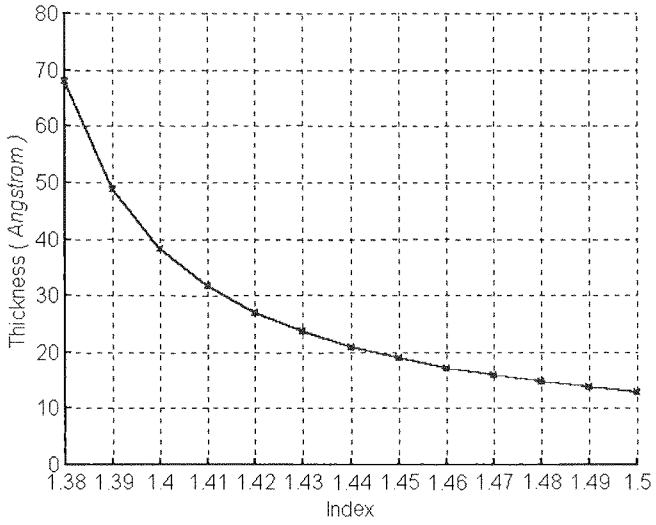

Fig.6. The evaluated thickness of the alkylthiol film as a function of its refractive index

5. Conclusions

The feasibility of a fiber-optic approach with promising potential in applications for investigating the properties of the metal surface or interface and its adsorbed film has been studied. Compared with ellipsometry, this means is rather easy to use and is capable of performing real-time detection. The advantages are evident as well over the bulk prism-based SPR system traditionally employed, because the fiber can be directly immersed into the thiol solution and the measurements can be carried out at a distance. Moreover, it should be underlined that the results obtained by this fiber-optic SPR arrangement are the spatially averaged values over an entire dielectric film, since the light rays propagating through the fiber hit almost whole uncladded part of the fiber. Otherwise, ellipsometry and the prism-based SPR system only provide information about a small area of the dielectric film on the metal surface where light beam illuminates it. For this reason, the fiber-optic SPR approach appears more adapted than ellipsometry and the prism-based SPR system to monitor the variations over entire investigated dielectric film.

By simple fiber-optic SPR experiments, the 3-step formation kinetics of the alkylthiol SAM has been monitored in real time and its static characteristics have been explored. To our knowledge, it is the first application of the fiber-optic SPR technique to study SAMs, and the first direct observation of the tilting process during the self-assembly of alkylthiol.

A similar method can be extended to the additional layers on the SAM surface, such as the coupled biochemical layers. Further attention is thus given to develop a biosensor based on fiber-optic SPR where the biological reactions can be detected in situ and the sizes of the antibody and antigen molecular films can be estimated.

Acknowledgements

The authors would like to thank our colleagues Professor Jean Rene MARTIN and Mr. Denis DESCHATRE for their contributions to the realization of thermal stabilization in the experiments. The control programs have been rewritten in C language on the basis of the original version developed by Mr. Frédéric CELL (TSI laboratory, Jean Monnet University in Saint-Etienne, France) whose contribution is also acknowledged.

References

1. I.Pockrand, Surface plasmon oscillations at silver surfaces with thin transparent and absorbing coatings, Surf. Sci., 72(1978) 577-588

2. W.P.Chen and J.M.Chen, Surface plasma wave study of submonolayer Cs and Cs-O covered Ag surfaces, Surf. Sci., 91(1980) 601-617

3. G. Kovacs, Optical excitation of surface plasmon-polaritons in layered media, Electromagnetic Surface Modes, Edited by A.D. Boardman, 1982 John Wiley & Sons Ltd. p.143-200

4. H.Sota, Y.Hasegawa and M.Iwakura, Detection of conformational changes in an immobilized protein using surface plasmon resonance, Anal. Chem., 70(1998) 2019-2024

5. G.B.Sigal, C.Bamdad, A.Barberis, J.Stominger and G.M.Whitesides, A self-assembled monolayer for the binding and study of histidine-tagged proteins by surface plasmon resonance, Anal. Chem., 68(1996) 490-497

6. L.S.Jung, C.T.Campbell, T.M.Chinowsky, M.N.Mar and S.S.Yee, Quantitative interpretation of the response of surface plasmon resonance sensors to adsorbed films, Langmuir, 14(1998) 5636-5648

7. L.H.Dubois and R.G.Nuzzo, Annu. Rev. Phys. Chem., 43(1992) 437

8. R.G.Nuzzo, F.A.Fusco and L.Allara, Spontaneously organized molecular assemblies. 3. Preparation and properties of solution adsorbed monolayers of organic disulfides on gold surfaces, J.Am.Chem.Soc, 109(1987) 2358-2368

9. M.D.Porter, T.B.Bright, D.L.Allara and C.E.D.Chidsey, Spontaneously organized molecular assemblies. 4. Structural characterization of n-alkyl thiol monolayers on gold by optical ellipsometry, infrared spectroscopy, and electrochemistry, J.Am.Chem.Soc, 109(1987) 3559-3568

10. M.Grunze, Preparation and characterization of self-assembled organic films on solid substrates, Physica Scripta., T49(1993) 711-717

11. T.W.Schneider and D.A.Buttry, Electrochemical quartz crystal microbalance studies of adsorption and desorption of self-assembled monolayers of alkyl thiol on gold, J.Am.Chem.Soc, 115(1993) 12391-12397

12. S.S.Cheng, D.A.Scherson and C.N.Sukenik, In situ observation self-assembly by FTIR/ATR, J.Am.Chem.Soc, 114(1992) 5436-5437

13. W.B.Lin, J.M.Chovelon, N.Jaffrezic-Renault, Fiber-optic surface plasmon resonance for determination of thickness and optical constants of thin metal films, Appl. Opt., Submitted

14. W.B.Lin, M.Lacroix, J.M.Chovelon, N.Jaffrezic-Renault, A.Trouillet, C.Veillas, H.Gagnaire, Development of a fiber-optic sensor based on surface plasmon resonance on silver film for monitoring aqueous media, Thin Solid Films., Submitted

15. D.R Lide, Handbook of Chemistry Physics, 71st ed.(1990), CRC Press

16. W.B.Lin, N.Jaffrezic, A.Gagnaire and H.Gagnaire, The effects of polarization of the incident light—modeling and analysis of a SPR multimode optical fiber sensor, Sens. Actuators A, Submitted

17. G.Hahner, Ch.Woll, M.Buck and M.Grunze, Investigation of intermediate steps in the self-assembly of n-alkanethiols on gold surfaces by soft X-ray spectroscopy, Langmuir, 9(1993) 1955-1958

18. A.Ulman, An introduction to ultrathin organic films, from Lagmuir-Blodgett to self assembled monolayers, Academic Press (1991).

Immunocapteurs intrinsèques à fibre optique basés sur l'excitation de la résonance de plasmon de surface par une lumière monochromatique

Résumé Article 5

Immunocapteurs intrinsèques à fibre optique basés sur l'excitation de la résonance de plasmon de surface par une lumière monochromatique

Le développement d'un biocapteur sans marqueur a suscité un intérêt considérable pour des applications à fort potentiel dans le diagnostic médical, l'analyse des aliments et le contrôle environnemental. Les instruments permettant de réaliser une détection immunologique directe et sans marqueur actuellement sur le marché mondial, sont uniquement les biocapteurs de la société Biacore (suède). Leur principe de fonctionnement est basé sur l'excitation et la détection de la résonance de plasmon de surface (SPR). Cependant ces dispositifs Biacore sont très chers. La sonde Biacore, un biocapteur à fibre optique, utilise une lumière polychromatique qui excite le SPR et un spectrographe pour mesurer la distribution spectrale de l'intensité lumineuse transmise. Nous proposons, dans cet article, un immunocapteur à fibre optique, dans une configuration différente dans laquelle une lumière monochromatique à la longueur d'onde de 658 nm émise par une diode laser commerciale est utilisée. Ainsi, le spectrographe est éliminé, ce système étant plus simple et meilleur marché.

La configuration de cette immunosonde à fibre optique est décrite dans cet article. Puis la région sensible par rapport à l'angle d'incidence externe est choisie en suivant l'analyse théorique. Les expériences de détection de l'interaction antigène-anticorps de l'IgG de lapin sont menées. La sensibilité et la spécificité de notre système à fibre optique sont examinées et comparées à la sonde Biacore. De plus, les paramètres optiques de la couche d'anticorps et de la couche anticorps-antigène sont déterminés à partir des réponses SPR.

Ce travail qui propose un dispositif optique et qui montre la faisabilité d'un nouveau type d'immunocapteur à fibre optique, constitue la première étape vers le développement d'une immunosonde portable pour des immunoessais sans marqueur.

Preface to article 5

Intrinsic Fiber-Optic Immunosensors Based on Monochromatic Light Excitation of Surface Plasmon Resonance

The development of a label free biosensor has attracted considerable interest for its great potential applications in medical diagnoses, food analyses and environmental monitoring. The instruments capable of performing a direct and label free immunological detection and available in the market in the world are only the Biacore (Sweden) biosensors. Their working principle is based on the excitation and detection of the surface plasmon resonance (SPR). However, the Biacore devices are very expensive. The BIACORE probe, a fiber-optic biosensor developed by Biacore Company, utilizes a polychromatic light to excite the SPR and a spectrograph to measure the spectral distribution of the transmitted light intensity. We propose in this paper a fiber-optic immunosensor in different configuration that is illuminated by a monochromatic light at 658nm wavelength emitted from a commercially available laser diode. Since the spectrograph is eliminated, this unit reveals simpler and cheaper.

The configuration of this fiber-optic immunoprobe is described in this paper, and then the sensitive region regarding the external incident angles is chosen by means of the theoretical analyses. Experiments are carried out to detect the rabbit IgG antibody-antigen binding. The sensitivity and the specificity of our fiber-optic unit are examined and compared to the BIACORE probe. Finally, the optical parameters of the antibody layer and the bound antibody-antigen layer are characterized according to their own SPR responses.

This work, which verifies the optical design and the feasibility of this new kind of fiber-optic immunosensor, provides a starting step towards the development of a portable immunoprobe for non-labeling immunoassay.

Intrinsic Fiber-Optic Immunosensors Based on Monochromatic Light Excitation of Surface Plasmon Resonance

Wen Bin LIN[a,b], Jean Marc CHOVELON[a,c], Monique LACROIX[a], Nicole JAFFREZIC-RENAULT[a,*]

[a] IFOS, Ecole Centrale de Lyon, 36 Avenue Guy de Collongue, BP163, 69131 Ecully Cedex, France

[b] Electronic Science Department, Nankai University, Tianjin, 30071, China

[c] LACE, Claude Bernard-Lyon 1 University, 69622 Villeurbanne, France

[*] ***Corresponding author:*** *Tel: +33 4 72186243; Fax: +33 4 78331577; Email: Nicole.Jaffrezic@ec-lyon.fr*

Abstract: Currently, the intrinsic fiber-optic immunosensors in common use are usually based on polychromatic light excitation of the surface plasmon resonance, such as the BIACORE Probe developed by Biacore company (Sweden). We propose in this paper a fiber-optic immunosensor in different configuration that is illuminated by a monochromatic light at 658nm wavelength emitted from a commercially available laser diode. Since the spectrograph is eliminated, our unit reveals simpler and cheaper. By immobilization of the rabbit IgG antibody molecules on the surface of the transducer, the practical detection of the corresponding antigens proves the sensitivity and specificity of our biosensor. This work provides a starting step towards the development of a portable immunoprobe for non-labeling immunoassay.

Keywords: *Surface plasmon resonance; Immunoprobe; Fiber-optic sensor; Rabbit immunoglobulin G; Immunoassay*

1. Introduction

In recent years, the development of immunosensors has attracted considerable interest for its great potential applications in medical diagnoses, food analyses and environmental monitoring[1]. By contrast to most of the sensitive immunoassays which are based on labeling of the monitored protein molecules, such as radioimmunoassay (RIA) and enzyme-linked immunosorbent assay (ELISA), the optical methods are capable of performing a direct and label free immunological detection[2]. Among them, the surface plasmon resonance (SPR)

optical immunosensors are especially remarkable for their rather high sensitivity to kinetic evaluation of the biomolecular interactions[3-10]. The representative devices of this kind of biosensors are the Biacore (Sweden) commercial units[11-12].

Usually the antibody molecules are immobilized on the surface of an immunosensor, acting as the "selectors". The corresponding antigens called target species will bind to the antibodies. The affinity reaction alters the optical properties of the antibody layer as an increase of its thickness and/or the refractive index that can be quantified by means of SPR technique.

SPR is a special electromagnetic wave on the metal-dielectric interface associated with collective electron oscillations within the metal film[13]. In certain conditions, a large part of incident light energy can transfer to the surface modes resulting in a dramatic decrease of the reflected light intensity. As a result, SPR manifests itself as an intensity minimum in the incident angle dependent reflectivity. Since the surface electromagnetic field is concentrated at the metal surface and decays exponentially as a function of distance into the adjacent mediums, SPR can be utilized as a very sensitive immunoprobe to the biomolecular interactions taking place in the proximity of the metal surface.

The fiber-optic SPR immunosensors offer a number of potential advantages such as the portability, compactness and flexibility[10] over the classical Kretschmann configuration biosensors where a coupling prism is included[3-9]. The BIACORE probe, a fiber-optic biosensor developed by Biacore company, utilizes a polychromatic light to excite the SPR and a spectrograph to measure the spectral distribution of the transmitted light intensity in order to determine the minimum dependence of the wavelength shifts[14].

In this paper we report on a simpler fiber-optic SPR immunoprobe. Starting with a description of its configuration, its sensitive region of the external incident angles is predicted by means of the theoretical analyses. Experiments are carried out to detect the rabbit IgG antibody-antigen binding where the antibodies are grafted on the surface of gold film deposited on the fiber core. The sensitivity and the specificity of our fiber-optic unit are examined. Finally, the optical parameters of the antibody layer and the bound antibody-antigen layer are characterized according to their own SPR responses alone.

2. Configuration of the immunoprobe

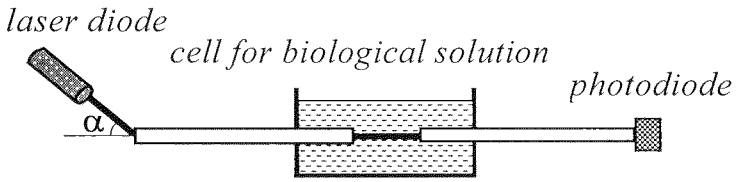

Fig.1. Diagram of the configuration of the fiber-optic immunosensor

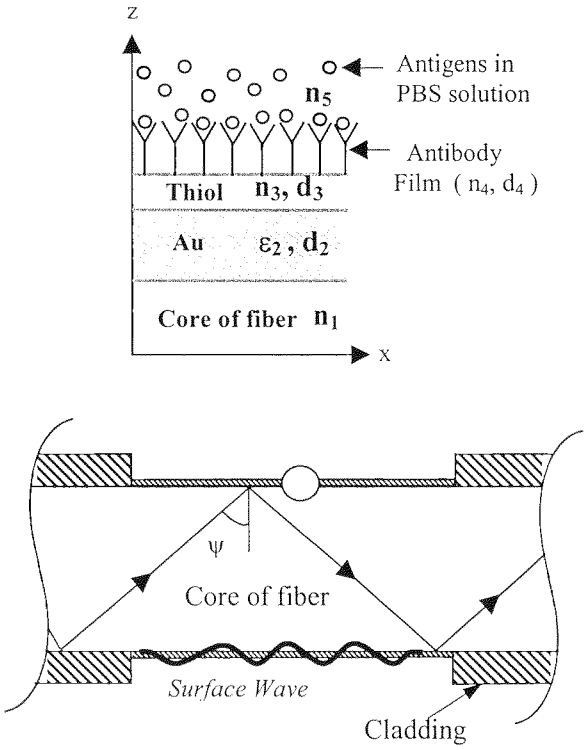

Fig.2. Diagram of the transducer in the fiber-optic immunosensor

Demonstrated in Fig.1 is a diagram of our fiber-optic immunosensor. A laser diode provides a parallel polarized monochromatic light beam to obliquely illuminate the input end of the fiber. The external incident angle is noted as α and the light wavelength of 658nm is

chosen so that the SPR may occur while the fiber is exposed to water. S- polarization with respect to the input end face of the fiber is adopted since this way is easier to keep a uniform light intensity on the incident face of fiber than p-polarization during the measurements of the sensing responses against different external incident angles. The intensity of the signal light is detected by a photodiode. The photovoltage was amplified, giving a reading proportional to the transmitted light power. By means of this system, the affinity reaction may be directly monitored by the variation of the output voltage values.

The transducer located on the uncladded part of the fiber consists of a gold film, an alkylthiol self-assembled monolayer (SAM) and an antibody layer which are consecutively deposited on the core of the fiber (see figure 2). The antibody layer makes the transducer capable of detecting the corresponding antigens in the biological solution. The internal incident angle for the light rays propagating in the fiber noted as Ψ must be greater than 75.0°, which is the critical angle determined by the refractive indices of the core (1.457) and the cladding (1.407), in order to keep the totally internal reflections.

3. Theoretical Analyses

The characterizations of the thin metal film and the alkylthiol SAM have been discussed in other papers[15,16]. Assuming that the two outermost mediums: core of fiber (n_1=1.457) and PBS (Phosphate Buffered Saline) solution (n_5=1.3358) are semi-infinite and that the 51nm thick gold layer (dielectric constants of ε_2=-13.15+i 1.34 at 658nm wavelength[15]) and the alkylthiol SAM (the thickness of d_3=1.77nm and the refractive index of n_3=1.463[16]) have been constructed, the antibodies immobilized on the thiol surface forming the fourth layer in figure 2 will alter the internally reflected light intensity. And the binding of the antigens to the antibodies will cause furthermore shifts of the curves of the internal incident angle dependence of reflectivity. In fact, the antibody film have to be formerly characterized so that the sensitive region of the external incident angle, at which the kinetics of the antibody-antigen binding can be monitored in real time with adequate sensitivity, can be determined. As will be reported below in the part of **4.4**, by measuring the SPR responses in PBS solution after the immobilization of the antibodies, the thickness of the antibody layer can be derived by best fitting the computed results to the experimental data as about 11nm if its refractive index is considered as 1.47[3]. Provided that the binding of the antigens to the antibodies makes a 2nm increase on the thickness of this biomolecular layer and its refractive index remains unchanged, the thickness variations from d_4=0 to 11nm then to 13nm correspond to three cases of this fourth layer as "without antibodies", "antibodies" and "antibodies

+antigens" respectively. The reflectivity at the core/metal interface is calculated by the method of matrix[17] since the multilayered configuration of the transducer can be almost exactly regarded as a one-dimensional planar 5-layered geometry[18]. The evolutions of the internal reflection curves are illustrated in figure 3.

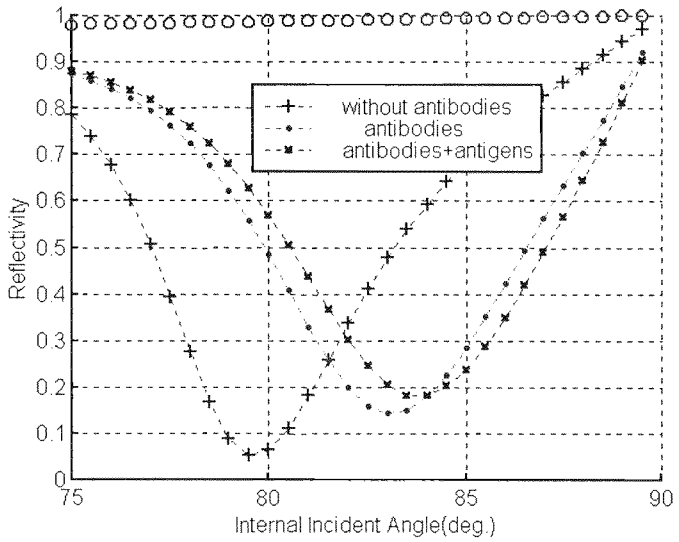

Fig.3. Computational reflectivity versus internal incident angle (ψ) for the 5-medium geometry. The dips in the curves above indicate the existence of the SPR. The variations of the biomolecular film (the fourth layer) are expressed as an increase of its thickness from d_4=0nm (without antibodies) to 11nm (antibodies) and then to 13nm (antibodies +antigens). The dotted curves refer to the incident light with p-polarization while the straight line of "o"s represents the results of s-polarized light incidence in the same conditions. Other parameters of n_1=1.457, ε_2=-13.15+i 1.34, d_2=51nm, n_3=1.463, d_3=1.77nm, n_4=1.47 and n_5=1.3358 are utilized in these calculations.

Our approach, having an important difference with BIACORE Probe, utilizes a parallel light beam emitted from a laser diode to directly illuminate the input end of the fiber, thereby obviating the bulk focus lens as used in BIACORE Probe. This fashion of light excitation results in a dispersion of the internal incident angle (Ψ) for the skew light rays in the fiber while the external incident angle (α) is fixed. These skew light rays propagate through the transducer with different trajectories and undergo different number of reflections, thus carry

different light power out of the fiber. The responses of this immunosensor can be obtained by accumulating the output light energy of all skew rays[18]. The variations of the biomolecular layer therefore can be related to the changes of the light power detected at the output end of the fiber. In figure 4, a sensitive region with regard to the external incident angle for monitoring the antibody-antigen reaction, is illustrated in the range between 12° and 21°.

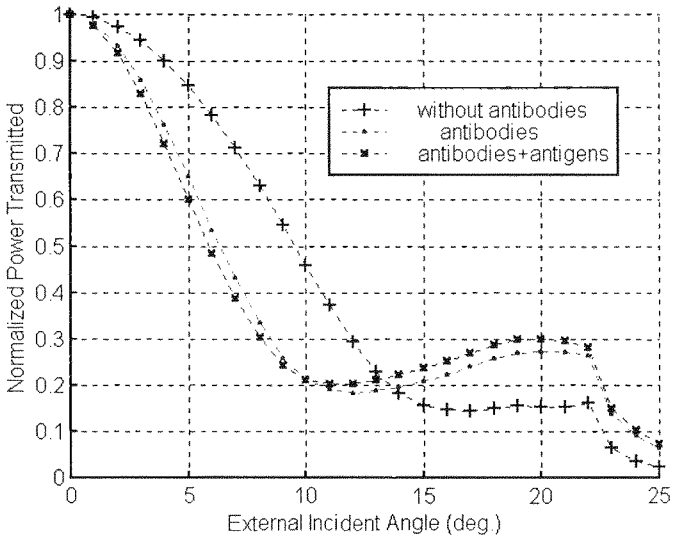

Fig.4. Computational normalized light power transmitted out of the fiber versus external incident angle α with d_4=0nm (without antibodies), 11nm (antibodies) and 13nm (antibodies +antigens) respectively. Other parameters used in these calculations are n_1=1.457, d_2=51nm, ε_2=-13.15+i 1.34, d_3=1.77nm n_3=1.463, n_4=1.47 and n_5=1.3358. In addition, s-polarization with respect to the input end of the fiber is adopted. The length of the fiber and the transducer are 210 and 15(mm) respectively and the refractive index of the cladding is assumed to be 1.407+ i 2.781×10^{-5} [15,16].

4. Experiments

4.1 Materials

Dimethylformamide (DMF), 1-ethyl-3-[3-(dimethylamino)propyl]carbodiimide (EDC), N-hydroxysuccinimide (NHS), goat anti-rabbit IgG, specific rabbit IgG, non specific sheep IgG and phosphate buffered saline tablets (PBS) were from Sigma-Aldrich. 11-Mercaptoundecanoic acid (alkylthiol) was synthesized at IBCP-CNRS Lyon, France. All other chemicals were of analytical grade.

4.2 Elaboration of the immunoprobe

4.2.1 Preparation of the fiber and the gold surface

The fiber used was multimode step-index silica/silicone optical fiber (Quartz et Silice PCS 600). A length of 21cm fiber was cut and its two ends were carefully polished to minimize the scattering of light. Part of the cladding, 15mm in length at the middle of the fiber, was removed with a sharp knife and then etched with sulfochromic treatment. A 51nm gold film monitored by the quartz-crystal detector was deposited on the fiber core via thermal evaporation. After 2 days of stabilization for the metal film exposed to air at room temperature, the fiber was immersed into the 1mM alkylthiol solution in ethanol. The homogeneity of the solution was kept with the help of a magnetic stirring system. An alkylthiol self-assembled monolayer (SAM) was constituted on the gold surface after 10 hour long reaction at the ambient temperature of 24°C[16]. The excess reagent was removed by rinsing with ethanol solution and then by an ultrasonic bath in pure water.

4.2.2 Immobilization of proteins

In the first step of the protein immobilization, the carboxylic acid-terminated alkylthiol SAM was exposed to the mixture consisting of 75mM DMF solution of EDC and 15mM water solution of NHS for 30 minutes. In the second step, the resultant of NHS ester monolayer was reacted for 30 minutes in the solution of antibodies (100μg/ml) diluted in a low-ionic-strength buffer (PBS, 10mM, pH7.4). After the blocking of the residual reactive groups with ethanolamine (1mM, pH8, one hour), the transducer was rinsed with distilled water and the fiber was kept in the PBS buffer.

4.3 Antibody-antigen binding

The fiber was mounted through a small cell where the biological solution was contained afterwards, and then it was installed to the experimental set-up (cf. Fig.1). The incident light was fixed at α=17° with s-polarization relative to the input end of the fiber. The 40ml PBS solution was injected into the small cell when timing began (t = 0). A magnetic stirring system was employed to keep the solution homogeneous. The environment temperature was maintained at a constant 24°C during the experiments. The reading of the voltage, which is proportional to the light power transmitted out of the fiber, was recorded every minute.

A 0.2ml specific rabbit IgG antigen solution with the concentration of 40μg/ml in PBS was successively injected into the small cell at t= 100, 145 and 190 minutes respectively, resulting in a progressive increase of the antigen concentrations in the 40ml BPS buffer corresponding to about 0.2, 0.4 and 0.6 μg/ml. The last injection of 0.6ml antigen solution at t=235minutes makes the antigen concentration in the small cell reach about 1.2μg/ml.

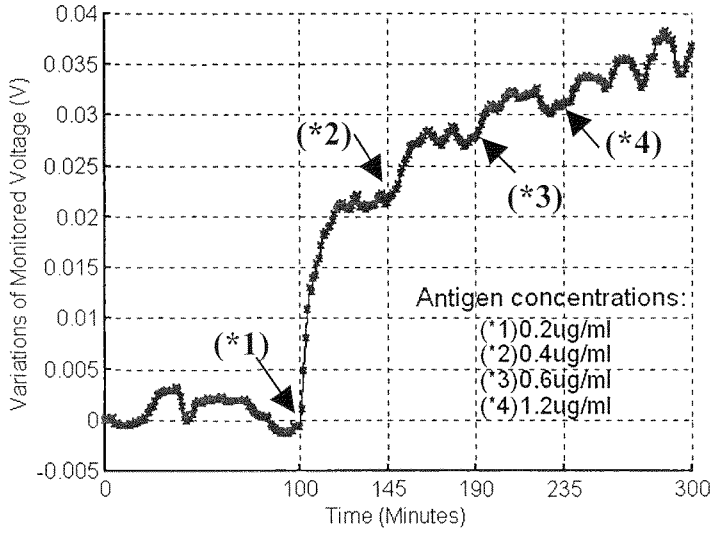

Fig.5. The time dependent variations of the monitored voltage present the kinetics of the immune reaction. Four successive injections of the specific antigens lead to the antigen concentrations in the detected PBS buffer of 0.2, 0.4, 0.6 and 1.2 μg/ml at the time of 100, 145, 190 and 235 minutes respectively.

The variations of the monitored voltage relative to its initial value (at t=0) are plotted in figure 5. The variations of the voltage between t=0 and 100 minutes present the noise level of the immunoprobe which is about 5 mV. This value, 3-4 times greater than the background noise of the system obtained after the formation of the alkylthiol SAM[16], strongly implies that the antibody film is not physically stable. The intervention of the water molecules to this protein layer affecting its dielectric properties[19] can presumably explain this phenomenon.

A notable ascend right after the first injection of the specific antigen molecules at t=100 minutes demonstrates that the antigen concentration as low as 0.2 μg/ml may already be detectable. The detection limit is thereby derived by referring to the noise level[20] as

70ng/ml. This quota seems to be better than that of the BIACORE Probe that is reported, for the typical detection limit of analyte, as greater than 1μg/ml (referred to BIACORE Probe Product Information, BR-9001-01 February 1997, published by Biacore company). A plateau, which reflects an equilibrium of the antigen-antibody reaction, is observed after exposure to the antigen solution for about 22 minutes. No remarkable increments of the detected light power are recorded as the results of the other successive injections, suggesting that the saturation has nearly been attained just after the first injection. In fact, it is difficult to compare our system with BIACORE Probe due to the different ways of operation in these two systems. Measurements by BIACORE Probe are based on an aspiration of only 0.1ml sample solution into a very small volume of the pipette tip. Otherwise in our system, the experiments are carried out in a very large sample volume, and a micro-agitator works, permitting a continuous furniture of the antigen molecules to the antibody surface until the steady static equilibrium is reached. Moreover, a relative low capacity of our biosensor for recognizing the antigens is related to its surface structure. The monolayer based antibody film is adopted in our immunoprobe while a matrix structure is used in BIACORE Probe[21].

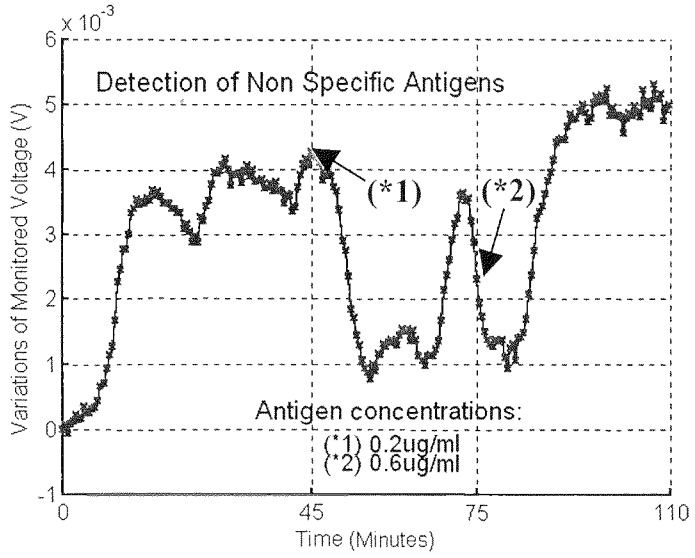

Fig.6. The time dependent variations of the monitored voltage present the detection of the non-specific antigens. Two successive injections of the non specific antigens lead to the antigen concentrations in the detected PBS buffer of 0.2 and 0.6 μg/ml at the time of 45 and 75 minutes respectively.

In addition, a compared fiber-optic immunosensor identical to the former one was exposed to the non specific sheep IgG solution. Two injections of this solution at t=45 and 75 minutes give the concentrations of the sheep IgG molecules in the PBS buffer as 0.2 and 0.6 μg/ml respectively. The experimental recordings, as it can be seen in figure 6, indicate that no significant and regular shifts of the detected light power by contrast to the noise level are observed. Thus the non-specific adsorption of the proteins onto the surface of the anti-rabbit IgG antibodies is negligible. The specificity of our fiber-optic SPR immunosensor is therefore verified.

4.4 Characterization of the biomolecular film

After the immobilization of the antibodies, the responses of the fiber-optic immunosensor were measured in PBS solution against the external incident angles (α). The thickness of this biomolecular layer is estimated by the best fit of the computational data to the experimental curve while its refractive index is set to be known as some possible values around 1.47[3]. The evaluated thickness of the antibody film as a function of the possible refractive index is plotted in figure 7. A thickness of 109Å, obtained for the refractive index of 1.47, is reasonable since it corresponds to a compact monolayer of the antibody molecules.

After the saturation of the affinity reaction, the fiber was rinsed and then re-exposed to PBS buffer. The biomolecular film after the antibody-antigen binding was assessed by measuring the SPR responses in PBS solution and by best fitting the calculated results to the experimental ones as explained above. The results are also illustrated in figure 7.

Notice that the results obtained by this fiber-optic SPR immunosensor are the effective and spatially average values over entire biomolecular film since the light rays propagating through the fiber hit almost whole uncladded part of the fiber[16]. Referred to figure 7, the effective and average thickness of the antibody layer is yielded as 109Å and after the binding of the antigens it augments to 129Å if its refractive index is assumed to remain unchanged as 1.47. As it has been underlined above, the evaluated thickness for the antibody film is commensurate to the scale of the rabbit anti-IgG molecular monolayer. And a 20Å growth in the thickness after the immune reaction proposes a surface coverage of only 40% for the antigen molecules if a complete rabbit IgG layer, defined as the 100% coverage as it has been measured in ref.3, should present a thickness of 50Å at the refractive index of 1.47. It is apparent that not all of the antibodies are appropriately oriented for binding.

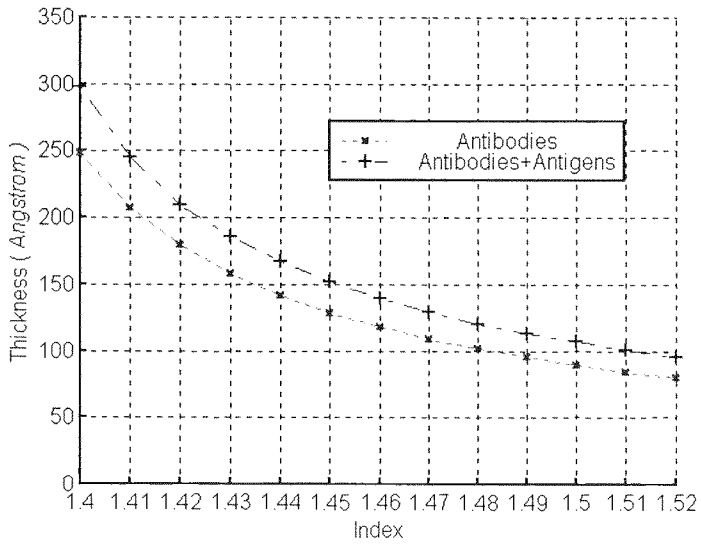

Fig.7. The evaluated thickness of the antibody film (marked as "x") and of the antibody-antigen binding film resulting from the immune reaction (marked as "+") as a function of its refractive index

5. Conclusions

A simple arrangement of our fiber-optic SPR immunosensor has manifested good performances in both sensitivity and specificity in comparison with the commercialized BIACORE Probe, which is much more complex and expensive. The optical conception and the feasibility of this fiber-optic SPR immunosensor have been validated by experiments. Further works can be contributed to improve and moreover optimize this immunoprobe on the basis of our firsthand data. This work makes progress towards future portable biosensors that become more and more attractive due to their vast potential in applications.

Acknowledgements

The authors would like to thank Professor Claude MARTELET for helpful discussion and Professor Jean Rene MARTIN and Mr. Denis DESCHATRE for contributions to the realization of the temperature controls in the experiments.

References

1. B.Hock, Antibodies for immunosensors, A review, Anal. Chim. Acta, 347(1997) 177-186

2. A.Brecht, G.Gauglitz, Label free optical immunoprobes for pesticide detection, Anal. Chim. Acta, 347(1997) 219-233

3. B.Liedberg, C.Nylander and I.Lundström, Surface plasmon resonance for gas detection and biosensing, Sensors and Actuators, 4(1983) 299-304

4. M.T.Flanagan and R.H.Pantell, Surface plasmon resonance and immunosensors, Electron Lett., 20(1984) 968-970

5. P.B.Daniels, J.K.Deacon, M.J.Eddowes and D.G.Pedley, Surface plasmon resonance applied to immunosensing, Sensors and Actuators, 15(1988) 11-18

6. R.P.H.Kooyman, H.Kolkman, J.Van Gent and J.Greve, Surface plasmon resonance immunosensors: sensitivity considerations, Anal. Chim. Acta, 213(1988) 35-45

7. E.Fontana, R.H.Pantell and S.Strober, Surface plasmon immunoassay, Appl. Opt., 29(1990) 4694-4704

8. M.C.Millot, F.Martin, D.Bousquet, B.Sébill and Y.Lévy, A reactive macromolecular matrix for protein immobilization on a gold surface. Application in surface plasmon resonance, , Sensors and Actuators, B29(1995) 268-273

9. R.W.Nelson, J.R.Krone and O.Jansson, Surface plasmon resonance biomolecular interaction analysis mass spectrometry. 1. Chip-based analysis, Anal. Chem., 69(1997) 4363-4368

10. R.W.Nelson, J.R.Krone and O.Jansson, Surface plasmon resonance biomolecular interaction analysis mass spectrometry. 2. Fiber optic-based analysis, Anal. Chem., 69(1997) 4369-4374

11. E.Stenberg, B.Persson, H.Roos and C.Urbaniczky, Quantitative determination of surface concentration of protein with surface plasmon resonance using radiolabeled proteins, J. Colloid and Interface Sci., 143(1991) 513-526

12. R.Karlsson, A.Michaelsson and L.Mattsson, Kinetic analysis of monoclonal antibody-antigen interactions with a new biosensor based analytical ayatem, J. Immuno. Meth., 145(1991) 229-240

13. H.Raether, Surface plasma Oscillations and their applications, Physics of Thin Films, Academic Press, New York, 9(1977) 145-261

14. R.C.Jorgenson and S.S. Yee, A fiber-optic chemical sensor based on surface plasmon resonance, Sensors and Actuators B, 12(1993) 213-220; More information about Biacore can be referred to the internet site: http://www.biacore.com

15. W.B.Lin, J.M.Chovelon, N.Jaffrezic-Renault, Fiber-optic surface plasmon resonance for determination of thickness and optical constants of thin metal films, Appl. Opt., Submitted

16. W.B.Lin, J.M.Chovelon, M.Lacroix, N.Jaffrezic-Renault, In situ observation and characterization of self-assembled monolayers by fiber-optic surface plasmon resonance, J. Chem. Phys., Submitted

17. K.Kurosawa, R.M.Pierce, S.Ushioda and J.C.Hemminger, Raman scattering and attenuated-total-reflection studies of surface-plasmon polaritons, Phys. Rev. B, 33(1986) 789-798

18. W.B.Lin, N.Jaffrezic-Renault, A.Gagnaire and H.Gagnaire, The effects of polarization of the incident light—modeling and analysis of a SPR multimode optical fiber sensor, Sens. Actuators A, Accepted

19. H.Sota, Y.Hasegawa and M.Iwakura, Detection of conformational changes in an immobilized protein using surface plasmon resonance, Anal. Chem., 70(1998) 2019-2024

20. L.A.Currie, Detection and quantification limits: origins and historical overview, Anal. Chim. Acta, 319(1999) 127-134.

21. S.Lofas and B.Johnsson, A novel hydrogel matrix on gold surface in surface plasmon resonance sensors for fast and efficient covalent immobilization of ligands, J.Chem.Soc.Chem.Commun.(1990), 1526-1528

MINISTERE DE L'EDUCATION NATIONALE,
DE LA RECHERCHE ET DE LA TECHNOLOGIE

ATTESTATION

DIPLOME DE DOCTEUR DE L'ECOLE CENTRALE DE LYON

(Arrêté du 30 Mars 1992)

Le Directeur de l'ECOLE CENTRALE DE LYON soussigné, certifie que

Monsieur LIN Wenbin

né(e) le 3 Février 1965 à FUJIAN (Chine)

a obtenu le **16 MARS 2000**

devant un jury composé de

P. BENECH	Professeur - LEMO, ENSERG-INPG - 23, rue des Martyrs - BP 257 - 38016 GRENOBLE
J.M. CHOVELON	Professeur - LACE - Université Claude Bernard - Lyon I - 69622 VILLEURBANNE Cedex
H. GAGNAIRE	Professeur - TSI - Université Jean Monnet - 23, rue du Docteur Paul Michelon 42023 SAINT-ETIENNE
N. JAFFREZIC	Directeur de Recherche CNRS - IFoS - Ecole Centrale de Lyon
O. PARRIAUX	Professeur - TSI - Université Jean Monnet - 23, rue du Docteur Paul Michelon 42023 SAINT-ETIENNE

le **GRADE DE DOCTEUR**

Ecole doctorale : **MATERIAUX**

Titre : ***Développement de capteurs à fibre optique basés sur la résonance de plasmon de surface pour la détection physique, chimique et biologique***

Avec la mention : **TRES HONORABLE AVEC FELICITATIONS**

Fait à Ecully, le 22 mars 2000

P/Le Directeur de l'E.C.L.
Le Directeur des Etudes et de la Pédagogie
Chargé des enseignements de spécialité

ECOLE CENTRALE DE LYON
SCOLARITE
3ème Cycle

A. NICOLAS

(IL NE PEUT ETRE DELIVRE DE DUPLICATA DE LA PRESENTE ATTESTATION. IL APPARTIENT A L'INTERESSE(E) D'EN ETABLIR DES COPIES QU'IL FERA CERTIFIER CONFORMES).